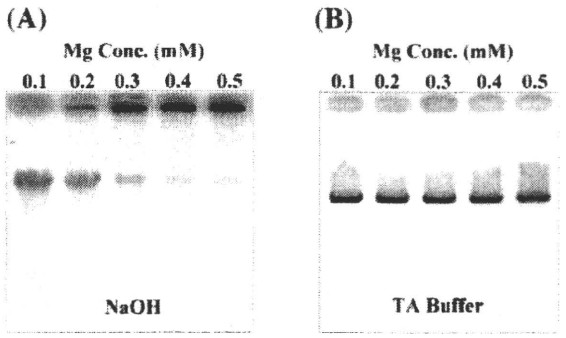

Fig. 3. Electrophoretic mobility shift of λ phage DNA (48 kbp) in the presence of $MgCl_2$. (A) 50 ng λ Phage DNA samples with 0.1-0.5 mM $MgCl_2$ were electrophoresed in TA (40 mM Tris-acetate) buffer, (B) 600 ng λ DNA samples with 0.1-0.5 mM $MgCl_2$ were electrophoresed in 50 mM NaOH.

Table 3. Effect of pretreatment of sample upon the retention of DNA on PNWF filter

DNA	BSA	Treatment	Threshold time[1] (min)
−	−	NaOH	NA[2]
+	−	NaOH	18.9 ± 1.0
+	+	NaOH	52.0 ± 9.3
+	+	Mg^{2+} + NaOH	18.2 ± 0.5
+	+	Mg^{2+} + NaOH → EDTA	18.4 ± 1.5
+	+	Mg^{2+} + EDTA → NaOH	NA

[1]: The time needed for the turbidity of each sample to exceed 0.1 at 650 nm with a real time turbid meter.
[2]: NA, amplification was not observed after 60 min.

DNA decreased by the addition of Mg^{2+} under alkaline conditions in a concentration-dependent manner. λ Phage DNA was condensed to the origin of the electrophoresis at the Mg^{2+} concentration of more than 0.3 mM (Fig. 3A). On the contrary, Mg^{2+} had no effect under neutral pH conditions (Fig. 3B). The efficient amplification of specific DNA fragments in the LAMP reaction rapidly increased turbidity caused by the formation of magnesium pyrophosphate. Table 3 shows the time for various samples to reach a turbidity of 0.1 at 650 nm in LAMP reactions for *N. gonorrhoeae*. Rapid amplification (18.9 min) was seen with the PNWF filter that adsorbed DNA in the presence of NaOH. A significantly delayed LAMP reaction time (52.0 min) was observed when 0.3 mg/ml BSA was added to the DNA/NaOH mixture. The LAMP reaction time was 18.2 min, similar to the time noted in the sample without BSA when 1 mM Mg^{2+} was added to the DNA/NaOH/BSA mixture. The addition of EDTA to the mixture of DNA with NaOH, BSA, and Mg^{2+} had no effect on LAMP reaction time (18.4 min). On the contrary, the addition of EDTA to the DNA sample with BSA and Mg^{2+} prior to alkaline treatment completely inhibited the effect of Mg^{2+} on DNA recovery, as no amplification of the specific DNA fragment was observed by LAMP. By these results, it became obvious that the presence of contaminating proteins in the DNA solution inhibited DNA retention on the PNWF filter, and the DNA-Mg^{2+} interaction under alkaline conditions caused strong complex formation and was not affected by contaminating proteins. This data was in close agreement with the condensation profile obtained by agarose gel electrophoresis (Fig. 4).

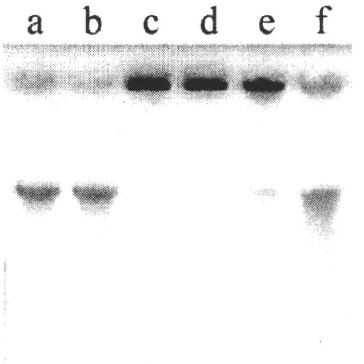

Fig. 4. Effect of NaOH on the electrophoretic mobility shift of DNA on agarose gel electrophoresis in the presence of BSA, Mg^{2+}, and EDTA. λ Phage DNA was treated as follows and analyzed on alkaline agarose gel electrophoresis. (a) NaOH, (b) BSA and NaOH, (c) $MgCl_2$ and NaOH, (d) BSA, $MgCl_2$, and NaOH, (e) 1 mM EDTA was added to (c) after NaOH treatment, and (f) 1 mM EDTA was added to (c) followed by NaOH treatment.

Table 4. Effect of Mg/NaOH method for condensation of extracted TB genome from specimens by using PNWF filter

No. of *M. tuberculosis* (CFU)	DNA purified by	
	PNWF-filter	Amplicor
40,000	+	+
8,000	+	+
1,600	+	+
320	+	+
64	+	−
12.8	−	−
2.56	−	−

Use of PNWF filter for the detection of *M. tuberculosis* in sputum: The applicability of PNWF filter for the detection of *M. tuberculosis* in sputum was examined using spiked sputum with serially diluted *M. tuberculosis*. The detection limit of *M. tuberculosis* by LAMP using PNWF filter method was shown to be 64 bacilli/200 μL sputum, whereas that using DNA extraction module in Amplicore *Mycobacteria*™ was 320 bacilli/0.2 mL sputum (Table 4). Alternatively, the detection limit for bacilli number by PNWF filter method was calculated to be 16 as 50 μL of freeze/thaw extract in a total volume of 100 μL was used for a reaction (Table 4). This was the same as for DNA extraction module in Amplicore *Mycobacteria*™ (as 5 μL from a total volume of 100 μL of DNA extract from 320 bacilli/0.2 mL sputum was used. In addition, this sensitivity was consistent with the data presented in previous publication on LAMP method for the detection of *M. tuberculosis* using the same primer set (11). This data demonstrated the efficient entrapment of DNA on PNWF filter in the presence of Mg^{2+} under alkaline conditions. The high sensitivity of 64 bacilli/200 μL sputum seemed

to be enough for the detection of *M. tuberculosis* not only from smear positive (usually more than 5,000 bacilli/mL sputum) but also from the many smear negative/tuberculosis culture positive sputum.

Divalent metal cations were known to interact with bases, sugar, and the phosphate group of DNA. In general, they bind to phosphate and stabilize double-stranded DNA at low concentrations, and to bases, and destabilize double-stranded DNA due to the cleavage of the hydrogen bond on the base pairs at high concentrations. Although some information is available as mentioned above, little investigation has been conducted on the interaction between DNA and Mg^{2+} under alkaline conditions since Mg^{2+} easily precipitates as $Mg(OH)_2$. The data presented in this study showed that DNA interacts with Mg^{2+} at lower concentrations (0.1–0.5 mM) under alkaline conditions where little precipitation of $Mg(OH)_2$ occurs. Electrophoretic DNA mobility reduction under such conditions suggested the possibility that DNA self-associates via Mg^{2+}.

The LAMP method emerged as a powerful tool for facilitating point-of-care genetic testing in place of the conventional PCR amplification (12–16) as it can be done under isothermal conditions ranging from 60°C to 65°C. Also, results can be obtained in a shorter time compared with PCR, making the LAMP method a very promising candidate. To increase the utility of the LAMP method in hospitals and primary care facilities, the DNA purification and concentration method from clinical specimens appears to be very important. Thus, the entrapment of DNA aggregate with Mg^{2+} under alkaline conditions on PNWF filter was examined as a rapid, simple, and low cost method. Sensitive detection of *M. tuberculosis* from decontaminated sputum by LAMP using PNWF filter in this study demonstrated the usefulness of this method for the diagnosis of tuberculosis in various medical settings.

Acknowledgments This study was supported partly by Grant-in-Aid for Program of Founding Research Center for Emerging and Re-emerging Infectious Diseases from the Ministry of Education, Culture, Sports, Science and Technology, Japan (MEXT) to YS, in part by the Global Center of Excellence (COE) Program, "Establishment of International Collaboration Centers for Zoonosis Control" from MEXT to YS, in part by Grant-in-Aid for Scientific Research from Japan Society for the Promotion of Science (JSPS) to YS and CN, Grant-in-Aid for "Science and Technology Research Partnership for Sustainable Developement" from Japan Science and Technology Agency (JST) to YS, and in part by a grant from U.S.-Japan Cooperative Medical Science Programs to YS.

REFERENCES

1. Boom, R., Sol, C.J.A., Salimans, M.M.M., et al. (1990): Rapid and simple method for purification of nucleic acids. J. Clin. Microbiol., 28, 495–503.
2. Nakatani, S.M., Burger, M., Assef, M.C., et al. (2004): Efficient method for mycobacterial DNA extraction in blood cultures aids rapid PCR identification of *Mycobacterium tuberculosis* and *Mycobacterium avium*. Eur. J. Clin. Microbiol. Infect. Dis., 23, 851–854.
3. Gosule, L.C. and Schellman, J.A. (1978): DNA condensation with polyamines I. Spectroscopic studies. J. Mol. Biol., 121, 311–326.
4. Wilson, R.W. and Bloomfield, V.A. (1979): Counterion-induced condensation of deoxyribonucleic acid. A light-scattering study. Bio. Chem., 18, 2192–2196.
5. Li., A.Z., Haiyan, H., Xiaodan, et al. (1998): A gel electrophoresis study of the competitive effects of monovalent counterion on the effect of divalent counterions binding to DNA. Bio. Phys. J., 74, 964–973.
6. Knight, J.D. and Adami, R.C. (2003): Stabilization of DNA utilizing divalent cations and alcohol. Int. J. Pharm., 264, 15–24.
7. Teeters, M.A., Root, T.W. and Lightfoot, E.N. (2004): Adsorption and desorption behavior of plasmid DNA on ion-exchange membranes. Effect of salt valence and compaction agents. J. Chromatogr. A., 1036, 73–78.
8. Conwell, C.C. and Hud, N.V. (2003): $MgCl_2$ enhances cluster formation by nanoscale toroidal DNA condensates. J. Cluster Sci., 14, 115–122.
9. Krakauer, H. (1974): A thermodynamic analysis of the influence of simple mono and divalent cations on the conformational transitions of polynucleotide complexes. Biochemistry, 13, 2579–2589.
10. Ayene, I.S., Koch, C.J. and Krisch, R.E. (2007): DNA strand breakage by bivalent metal ions and ionizing radiation. Int. J. Radiat. Biol., 83, 195–210.
11. Pandey, B.D., Poudel, A., Yoda, T., et al. (2008): Development of an in-house loop-mediated isothermal amplification (LAMP) assay for detection of *Mycobacterium tuberculosis* and evaluation in sputum samples of Nepalese patients. J. Med. Microbiol., 57, 439–443.
12. Notomi, T., Okayama, H., Masubuchi, H., et al. (2000): Loop-mediated isothermal amplification of DNA. Nucleic Acids Res., 28, E63.
13. Mori, Y., Nagamine, K., Tomita, N., et al. (2001): Detection of loop-mediated isothermal amplification reaction by turbidity derived from magnesium pyrophosphate formation. Biochem. Biophys. Res. Commun., 289, 150–154.
14. Nagamine, K., Watanabe, K., Ohtsuka, et al. (2001): Loop-mediated isothermal amplification reaction using nondenatured template. Clin. Chem. 47, 1742–1743.
15. Nagamine, K., Hase, T. and Notomi, T. (2002): Accelerated reaction by loop-mediated isothermal amplification using loop primers. Mol. Cell. Probes, 16, 223–229.
16. Nagamine, K., Kuzuhara, Y. and Notomi, T. (2002): Isolation of single-stranded DNA from loop-mediated isothermal amplification products. Biochem. Biophys. Res. Commun., 290, 1195–1198.

Jpn. J. Infect. Dis., 63, 412-416, 2010

Original Article

Possible Mode of Emergence for Drug-Resistant Leprosy Is Revealed by an Analysis of Samples from Mexico

Masanori Matsuoka*†, Yasuhiko Suzuki[1,2†], Iris Estrada Garcia[3], Mary Fafutis-Morris[4], Alberto Vargas-González[5], Cristina Carreño-Martinez[6], Yukari Fukushima[1], and Chie Nakajima[1]

Leprosy Research Center, National Institute of Infectious Diseases, Tokyo 189-0002;
[1]Department of Global Epidemiology, Hokkaido University Research Center for Zoonosis Control, Sapporo 001-0021;
[2]Science and Technology Research Partnership for Sustainable Development, Japan Science and Technology/Japan International Cooperation Agency, Tokyo 102-0081, Japan;
[3]National School of Biological Science, IPN, Mexico;
[4]CIINDE Department of Physiology, CUCS, University of Guadalajara, Guadalajara;
[5]CIR "Dr. Hideyo Noguchi", University Autonomous of Yucatan, Yucatan; and
[6]Leprosy Department, Mycobacterial Disease Prevention Programs, CENAVECE, Mexico, Mexico

(Received July 14, 2010. Accepted September 24, 2010)

SUMMARY: Mexico is a country with sporadic leprosy cases, and the reemergence of drug resistance is a concern. In this study, molecular analysis of *Mycobacterium leprae* was employed to clarify the spread of drug-resistant leprosy. Thus, drug resistance-determining regions in the *folP1*, *rpoB*, and *gyrA* genes, which are associated with resistance to dapsone, rifampicin, and ofloxacin, respectively, were analyzed by direct sequencing of the PCR product. No mutations in the *folP1* gene were observed in any of the 72 slit skin samples obtained from 38 patients, although two samples carrying a mutation at codon 425 in the *rpoB* gene, which confers resistance to rifampicin, a key component of multidrug therapy, were identified. In addition, a mutation at codon 91 in the *gyrA* gene, which correlates with ofloxacin resistance, was found in one sample. These results demonstrate the existence of rifampicin- and ofloxacin-resistant leprosy. Interestingly, wild-type and mutant sequences in the *gyrA* gene were found to coexist in one clinical sample. In addition, all three drug resistance-related mutations were found in only one of the two earlobes of the patients concerned, suggesting a possible pathway for the spread of drug-resistant *M. leprae*.

INTRODUCTION

Multidrug therapy (MDT) (1) has been used widely since 1984 and still plays a pivotal role in the treatment of leprosy. Combination therapy with rifampicin, clofazimine, and dapsone is recommended for the treatment of multibacillary leprosy, whereas therapy with rifampicin and dapsone is recommended for the treatment of paucibacillary leprosy. Ofloxacin plays a key role in the treatment of single-lesion cases and drug-resistant leprosy. The number of leprosy patients with drug-resistant *Mycobacterium leprae* has increased due to therapeutic failure or low compliance (2,3). Although drug-susceptibility tests are known to give better outcomes in the treatment of leprosy, they are generally not performed in the great majority of high-burden countries since an in vitro drug-susceptibility test is not available. Current tests still rely on time-consuming and tedious methods that examine the growth of *M. leprae* in mouse footpads (4). This has hampered the undertaking of the comprehensive survey that would be required to evaluate the efficacy of MDT for controlling the spread of drug-resistant strains.

A recent extensive genetic analysis of drug-resistant *M. leprae* clarified the molecular basis of drug resistance in this organism and demonstrated the close tight correlation of dapsone, rifampicin, and ofloxacin resistance with mutations in the *folP1* (5-11), *rpoB* (7-10,12-16), and *gyrA* (7-9,12-16) genes, respectively. All mutations linked to drug resistance were found to occur in a specific region in each gene, the so-called drug resistance-determining region (DRDR). The sequence analysis of DRDRs in the *rpoB*, *gyrA*, and *folP1* genes of *M. leprae* is known to be a useful predictor of resistance that could eventually replace the mouse footpad method (10,16).

A surveillance of drug-resistant *M. leprae* strains using this methodology has been conducted in four countries (Myanmar, the Philippines, Indonesia, and India) to determine the prevalence in each country (10,17). Mexico is a country with sporadic leprosy where 143 new cases were detected in 2008 (18). However, only one dapsone-resistant case with relapse has been reported to date (19), and no comprehensive data on the level of drug-resistant leprosy cases are available in this country. We therefore analyzed mutations in the DRDRs of the *rpoB*, *gyrA*, and *folP1* genes of *M. leprae* by sequencing to investigate the prevalence of drug-resistant leprosy cases in Mexico. The importance of analyzing the

*Corresponding author: Mailing address: Leprosy Research Center, National Institute of Infectious Diseases, 4-2-1, Aobacho, Higashimurayama, Tokyo 189-0002, Japan. Tel: +81-423-91-8211, Fax: +81-423-94-9092, E-mail: matsuoka@nih.gp.jp

†These two authors contributed equally to this study.

DRDRs of *M. leprae* in multiple loci in a patient will also be discussed in this report.

MATERIALS AND METHODS

Sample collection: Samples from 38 patients undergoing MDT and living in western and southern Mexico were investigated (patient characteristics are shown in Table 1). Samples were obtained from earlobes or lesions by the slit skin method according to standard procedures recommended by the World Health Organization (20).

DNA preparation: Template DNA for PCR was prepared from slit skin samples as described elsewhere (10,21). Briefly, a blade containing bacilli from tissue on the edge was soaked in 70% ethanol and kept at room temperature until DNA preparation. Ethanol was removed from the samples by washing with phosphate-buffered saline (PBS, pH 7.2), then the samples were treated overnight with lysis buffer at 60°C and heated for 10 min at 95°C.

Table 1. Profiles of patients investigated in this study

Patient no.	Classification	Duration of MDT (mo)
1	MB	16
2	MB	12
3	MB	12
4	MB	17
5	MB	4
6	MB	13
7	MB	19
8	MB	4
9	MB	15
10	PB	2
11	MB	0
12	MB	8
13	MB	13
14	MB	14
15	MB	13
16	MB	22
17	MB	17
18	MB	12
19	MB	18
20	PB	2
21	MB	61
22	MB	15
23	MB	15
24	MB	7
25	MB	30
26	MB	32
27	MB	NR
28	MB	20
29	MB	28
30	MB	31
31	MB	20
32	MB	NR
33	MB	20
34	MB	13
35	MB	NR
36	MB	28
37	MB	140
38	MB	130

Median value of the treatment is 23.5 months. MDT, multidrug therapy; MB, multibacillary leprosy; PB, paucibacillary leprosy; NR, no record.

Detection of mutations in DRDRs: PCR for the amplification of DRDR-containing DNA fragments was performed with identical primers to those described previously using the Failsafe PCR System (EPICENTRE, Madison, Wis., USA) with a 25-μl reaction volume (10). The PCR products were purified and sequenced according to a protocol as described previously (9) using the ABI Prism BigDye™ Terminator v1.1 Cycle Sequencing Kit and the ABI Prism 3100XL Genetic Analyzer (Applied Biosystems, Foster City, Calif., USA) according to the manufacturer's instructions. The nucleotide sequences of the DRDRs in the *folP1*, *rpoB*, and *gyrA* genes were examined.

Cloning of PCR products and sequencing: The 130-bp PCR product of the *gyrA* gene was cloned into the vector pCR4-TOPO using the TOPO TA Cloning Kit for Sequencing (Invitrogen, Carlsbad, Calif., USA) according to the manufacturer's instructions. *Escherichia coli* host strain TOP10 cells (Invitrogen) were transformed and spread onto selective plates containing 100 μg/ml kanamycin and incubated at 37°C overnight. The cloned PCR products were amplified directly from *E. coli* colonies with primers M13F (5′-GTAAAAC GACGGCCAG-3′) and M13R (5′-CAGGAAACAG CTATGAC-3′) designated in the vector pCR4-TOPO, and the nucleotide sequences of the purified PCR products were determined as described above using the same primers.

Ethical approval: This study was approved by the institutional ethics committee of the National Institute of Infectious Diseases, Japan, and the corresponding Mexican institutional review boards. Slit skin smear samples were collected after informed consent had been obtained.

RESULTS AND DISCUSSION

Mutations in DRDRs: The detection of mutations in the DRDRs of the genes associated with resistance is a simple and reliable method for rapidly determining the drug susceptibility of *M. leprae*. Mutations at codons 53 and 55 in *folP1*, codons 407, 410, 420, 425, and 427 in *rpoB*, and codons 89 and 91 in *gyrA* have been found to be associated with resistance to dapsone (5–11), rifampicin (7–10,12–16), and ofloxacin (7–9,12–16), respectively, by comparing the results of drug-susceptibility tests with mice and mutation detection in the DRDR for each drug. This process enables a comprehensive analysis of the spread of drug-resistant leprosy and can be used to evaluate the efficacy of chemotherapy. In this study, the sequencing of DRDR-containing PCR products was applied to a number of samples from Mexican patients to analyze the prevalence of drug-resistant leprosy cases. Suitable PCR products were successfully obtained from all 72 samples taken from the 38 patients included in this study, thus indicating that slit skin smear samples from ear lobes are suitable for subsequent PCR amplification of DRDRs. The amplified DRDR PCR products were sequenced directly to determine the amino acid substitutions as summarized in

Table 2. Deduced amino acid substitutions found in *M. leprae* in the earlobes of patients

Patient no.	Duration of MDT (mo)	*folP1*		*rpoB*		*gyrA*	
		Left[1]	Right[1]	Left	Right	Left	Right
3	12	WT	WT[2]	S425L	WT	WT	WT
5	4	WT	WT	WT	WT	WT	A91V[3]
16	22	WT	WT	WT	S425L	WT	WT
17	17	WT	WT	G428S[4]	WT	WT	WT

[1]: Left and right exhibit left earlobe and right earlobe, respectively.
[2]: WT, wild type (without any mutations in DRDR).
[3]: Both wild type and mutant sequences were found in slit skin sample from one earlobe.
[4]: This mutation has not been reported to have a correlation with rifampicin resistance.

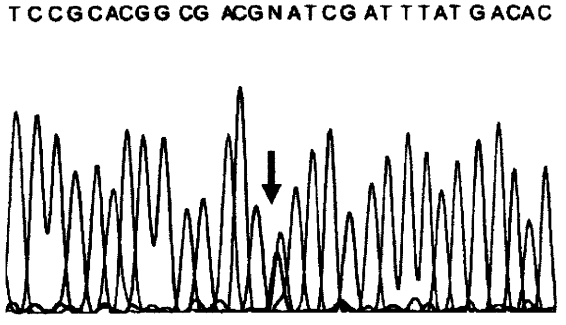

Fig. 1. Mixed sequence found in *gyrA* DRDR from a patient. Raw data from the ABI Prism 3100XL Genetic Analyzer was presented. Sequencing results suggested coexistence of wild type and mutant at codon 91 (GCA and GTA; conferring A91V substitution) nucleotide sequences in the *gyrA* gene. Arrow indicates the position of mixed bases.

Table 2. In consequence, no samples containing mutations in the DRDR of the *folP1* gene were found. On the contrary, a mutation at codon 425 (TCG: Ser to TTC: Leu) and another at codon 428 (GGC: Gly to AGC: Ser) of the *rpoB* gene were observed in one of two earlobes from one and two patients, respectively. Several previous studies have found that a mutation at codon 425 is associated with rifampicin resistance (7-10,12-16). A mutation at codon 428 has not been found in either *M. leprae* or *M. tuberculosis*, therefore the correlation between this mutation and rifampicin resistance remains unclear. Furthermore, the clinical data for this patient did not show any indication of rifampicin resistance. The correlation between this mutation at codon 428 and rifampicin resistance in *M. leprae* should be examined more clearly in a future study. Interestingly, all mutations were found in one of the earlobes but not both, the first such finding for leprosy patients. A mixed sequence of wild type and mutation (GCA: Ala and GTA: Val) at codon 91, which confers ofloxacin resistance (7-9, 12-16), was found in the PCR product of the *gyrA* DRDR in one of two earlobes from a lepromatous leprosy patient (Fig. 1). This was confirmed by sequencing 12 cloned PCR fragments and suggests that the sample contained both ofloxacin-susceptible and -resistant *M. leprae*. Although the coexistence of wild-type and mutant strains has been observed in *M. tuberculosis* (22), this is the first such example for *M. leprae*. If susceptibility is examined by the mouse footpad method for this case, growth should be observed in the mouse footpads treated with ofloxacin and identified to be resistant.

Table 3. Comparison of the prevalence of drug resistance in *M. leprae* in Mexico with those from other countries

Country	No. infected/no. tested (%)			Reference
	Dapson	Rifampicin	Quinolones	
Mexico	0/38 (0)	2/38 (5.3)	1/38 (2.6)	This work
Indonesia	1/121 (0.8)	4/121 (3.3)	ND	10
Myanmar	4/54 (7.2)	1/54 (1.8)	0/54 (0)	10
The Philippines	2/77 (2.6)	0/77 (0)	0/77 (0)	10
India	7/265 (2.6)	4/265 (1.5)	ND	23

ND, not done.

Prevalence of drug-resistant *M. lepraei* in Mexico: This is the first study to analyze the levels of drug-resistant leprosy in Mexico. The prevalence of dapsone-, rifampicin-, and ofloxacin-resistant *M. leprae* was calculated to be 0 (0/38), 5.3 (2/38), and 2.6% (1/38), respectively (Table 3), thus differing slightly from the previous studies undertaken in three Southeast Asian (Myanmar, the Philippines, and Indonesia) and one South Asian (India) countries, which revealed a higher level of dapsone resistance in both newly detected patients and intractable or relapsed cases, with no cases of ofloxacin resistance (10,23). This lower incidence of dapsone-resistant *M. leprae* was observed despite the use of dapsone monotherapy for more than 30 years before the introduction of MDT in Mexico. On the contrary, two apparently rifampicin-resistant strains of *M. leprae* were identified from intractable or relapsed cases (treatment duration >4 months). This higher number of rifampicin-resistant cases might be a result of MDT or other events. In addition, an ofloxacin-resistant *M. leprae* strain was found in one patient (treatment duration ≧4 months) even though this drug has not officially been used for the treatment of leprosy in Mexico. The prevalence of rifampicn-resistant *M. leprae* was slightly higher than in the four countries studied previously (Table 3).

As rifampicin and ofloxacin are key components in the chemotherapy of leprosy (26), and the spread of resistant *M. leprae* is likely to threaten current leprosy control strategies, careful observation needs to be continued. Furthermore, to prevent the reemergence of drug-resistant leprosy, accurate data regarding such cases should be collected by performing a longitudinal survey over an extensive area. The suspected incorrect usage of key drugs for leprosy in Mexico, as mentioned briefly above, further emphasizes the need for such control.

Mode of emergence of drug-resistant *M. leprae*: The emergence of ofloxacin-resistant *M. leprae* was revealed by the existence of *a* mutation in the quinolone resistance-determining region (QRDR) of the *gyrA* gene in a recent case (treatment duration up to 4 months). This patient had received MDT for 4 months (Table 2) and not been treated with any quinolones before sample collection. The *M. leprae* strain in this patient was therefore proposed to have acquired the resistant phenotype before initiation of the MDT. Rifampicin-resistant *M.*

leprae strains were also found in two patients. Interestingly, these strains were found to be single drug resistant, though the patients had received the standard MDT regimen for 12 and 22 months, respectively. Previous anti-tuberculosis treatment might have contributed to the emergence of rifampicin single-resistant *M. leprae*, since rifampicin is the only drug commonly used in MDT for both tuberculosis and leprosy. However, these patients with rifampicin-resistant *M. leprae* had no history of anti-tuberculosis therapy. Another explanation for the emergence of such cases, even after long-term treatment, might involve the current MDT regimen. In this regimen, as the daily components of MDT (dapsone and clofazimine) are self-administered whereas rifampicin is administered by a health care professional, the patients may have taken incorrect doses of daily components, thereby resulting in what would effectively be rifampicin monotherapy. Alternatively, the ready availability of therapeutic agents from drug stores might contribute to the emergence of single resistance to rifampicin and to ofloxacin as these drugs are also used to treat other infectious diseases. Indeed, numerous antibiotics, including rifampicin and ofloxacin, can be purchased from drug stores in Mexico without a prescriptions. Thus, single drug-resistant leprosy may emerge when people suffering from leprosy without being aware of take rifampicin or ofloxacin to treat other infectious diseases. These single drug-resistant *M. leprae* strains may have already been killed in the lesion by MDT, although the dead bacilli would remain at the sampling site and would subsequently act as a source of amplification of rifampicin resistance-determining region (RRDR) and QRDR by PCR. It is known that bacterial index (24) decreases by only one degree after 1 year's MDT in many cases (25).

It should also be noted that all the rifampicin-resistant *M. leprae* strains were found in only one earlobe of the patients concerned (Table 2). This suggests that drug-resistant *M. leprae* emerge in a single lesion and that these resistant bacilli then spread to other parts of the body. The coexistence of ofloxacin-susceptible and -resistant *M. leprae* in an earlobe, as described above, strongly supports this proposal.

As the results of this study suggest that the emergence of drug-resistant *M. leprae* may occur at one lesion site and the resistant bacilli spread to others, the detection of mutations in the DRDRs of *M. leprae* from multiple lesion sites in each patient is highly recommended in order to detect those patients infected with drug-resistant *M. leprae*. This would be important for both monitoring and preventing the spread drug-resistant *M. leprae* strains. Chemotherapy using drugs selected after drug-susceptibility tests can result in effective treatment without adverse reactions. However, as the conventional method based on the growth of *M. leprae* in mouse footpads is not practical as a drug-susceptibility test for large numbers of patients, DRDR sequence analysis may prove to be a viable alternative. In addition, a novel DNA microarray-based method for the detection of those mutations associated with drug resistance in *M. leprae* (27) may enable the comprehensive monitoring of these strains.

Acknowledgments This study was supported by the following grants: a grant from the Japan International Cooperation Agency to AVG; a Health Research Grant of Emerging and Re-emerging Infectious Diseases, Ministry of Health, Labour and Welfare of Japan to MM; partly by a grant from the International Medical Center, Ministry of Health, Labour and Welfare of Japan to MM; a grant from U.S.-Japan Cooperative Medical Science Program to MM and YS; and in part by the Global Center of Excellence (COE) Program "Establishment of International Collaboration Centers for Zoonosis Control", Ministry of Education, Culture, Sports, Science and Technology of Japan (MEXT), as well as Grants-in-Aid for the Program of Founding Research Center for Emerging and Re-emerging Infectious Diseases from MEXT to YS.

Conflict of interest None to declare.

REFERENCES

1. World Health Organization (1982): Chemotherapy of leprosy for control programs. WHO Tech. Rep. Series, 675. World Health Organization, Geneva.
2. Kyaw, K. and Aye, K.S. (2006): Case of multi-drug resistant leprosy-relapse or re-infetion. Myanmar J. Cur. Med. Pract., 10, 41-43.
3. Norman, G., Joseph, G., Ebenezer, G., et al. (2003): Secondary rifampin resistance following multi-drug therapy—a case report. Int. J. Lepr. Other Mycobact. Dis., 71, 18-21.
4. Shepard, C.C. (1960): The experimental disease that follows the injection of human leprosy bacilli into foot-pads of mice. J. Exp. Med., 112, 45-54.
5. Cambau, E., Carthagena, L., Chauffour, A., et al. (2006): Dihydropteroate synthase mutations in the *folP1* gene predict dapsone resistance in relapsed cases of leprosy. Clin. Infect. Dis., 42, 238-241.
6. Kai, M., Matsuoka, M., Nakata, N., et al. (1999): Diaminodiphenylsulfone resistance of *Mycobacterium leprae* due to mutations in the dihydropteroate synthase gene. FEMS Microbiol. Lett., 177, 231-235.
7. Maeda, S., Matsuoka, M., Nakata, N., et al. (2001): Multidrug resistant *Mycobacterium leprae* from patients with leprosy. Antimicrob. Agents Chemother., 45, 3635-3639.
8. Matsuoka, M., Kashiwabara, Y. and Namisato, M. (2000): A *Mycobacterium leprae* isolate resistant to dapsone, rifampin, ofloxacin and sparfloxacin. Int. J. Lepr. Other Mycobact. Dis., 68, 452-455.
9. Matsuoka, M., Kashiwabara, Y., Liangfen, Z., et al. (2003): A second case of multidrug resistant *Mycobacterium leprae* isolated from a Japanese patient with relapsed lepromatous leprosy. Int. J. Lepr. Other Mycobact. Dis., 71, 240-243.
10. Matsuoka, M., Budiawan, T., Aye, K.S., et al. (2007) The frequency of drug resistance mutations in *Mycobacterium leprae* isolates in untreated and relapsed leprosy patients from Myanmar, Indonesia and the Philippines. Lepr. Rev., 78, 343-352.
11. Williams, D.L., Spring, L., Harris, E., et al. (2000): Dihydropteroate synthase of *Mycobacterium leprae* and dapsone resistance. Antimicrob. Agents Chemother., 44, 1530-1537.
12. Cambau, E., Perani, E., Guillemin, I., et al. (1997): Multidrug-resistance to dapsone, rifampicin, and ofloxacin in *Mycobacterium leprae*. Lancet, 349, 103-104.
13. Cambau, E., Bonnafous, P., Perani, E., et al. (2002): Molecular detection of rifampicin and ofloxacin resistance for patients who experience relapse of multibacillary leprosy. Clin. Infect. Dis., 34, 39-45.
14. Honore, N. and Cole, S.T. (1993): Molecular basis of rifampin resistance in *Mycobacterium leprae*. Antimicrob. Agents Chemother., 37, 414-418.
15. Ramaswamy, S. and Musser, J.M. (1998): Molecular genetic basis of antimicrobial agent resistance in *Mycobacterium tuberculosis*. 1998 update. Tuber. Lung Dis., 79, 3-29.
16. Williams, D.L. and Gillis, T.P. (2000): Molecular detection of resistance in *Mycobacterium leprae*. Lepr. Rev., 75, 118-130.
17. You, E.Y., Kang, T.J., Kim, S.K., et al. (2005): Mutations in genes related to drug resistance in *Mycobacterium leprae* isolates from leprosy patients in Korea. J. Infect., 50, 6-11.
18. World Health Organization (2009): Global leprosy situation, 2009. Wkly. Epidemiol. Rec., 84, 333-340.

19. Lopez-Roa, R.I., Faftis-Morris, M. and Matsuoka, M. (2006): A drug resistant leprosy case detected by DNA sequencing analysis from a relapsed Mexican leprosy patient. Rev. Latinoam. Microbiol., 48, 256-259.
20. World Health Organization (1987): Laboratory Techniques for Leprosy. p. 65-66. WHO/COS/LEP/86.4.
21. de Wit, M.Y., Douglas, J.T., McFadden, J., et al. (1993): Polymerase chain reaction for detection of *Mycobacterium leprae* in nasal swab specimens. J. Clin. Microbiol., 32, 502-506.
22. Mokrousov, I., Otten, T., Manicheva, O., et al. (2008): Molecular characterization of ofloxacin-resistant *Mycobacterium tuberculosis* strains from Russia. Antimicrob. Agents Chemother., 52, 2937-2939.
23. Ebenezer, G.J., Norman, G., Joseph, G.A., et al. (2002): Drug resistant-*Mycobacterium leprae*—results of mouse foot pad studies from a laboratory in south India. Indian J. Lepr., 74, 301-312.
24. World Health Organization. Microbiology of *M. leprae*. Available at <http://www.who.int/lep/microbiology/en/>.
25. Kumar, A., Girdhar, A. and Girdhar, B.K. (2003): Pattern of bacillary clearance in multibacillary leprosy patients with multidrug therapy. Acta Leprol., 12, 123-128.
26. WHO Expert Committee on Leprosy (1998): Seventh report. Technical Report Series, 847. World Health Organization, Geneva.
27. Matsuoka, M., Aye, K.S., Kyaw, K., et al. (2008): A novel method for simple detection of mutations conferring drug resistance in *Mycobacterium leprae*, based on a DNA microarray, and its applicability in developing countries. J. Med. Microbiol., 57, 1213-1219.

International Immunology, Vol. 22, No. 12, pp. 915–925
doi:10.1093/intimm/dxq446
Advance Access publication 3 November 2010

PD-1–PD-L1 pathway impairs T_h1 immune response in the late stage of infection with *Mycobacterium bovis* bacillus Calmette–Guérin

Shunsuke Sakai[1], Ikuo Kawamura[1], Taku Okazaki[2], Kohsuke Tsuchiya[1], Ryousuke Uchiyama[3] and Masao Mitsuyama[1]

[1]Department of Microbiology, Kyoto University Graduate School of Medicine, Yoshida Konoe-cho, Sakyo-ku, Kyoto 606-8501, Japan
[2]Division of Immune Regulation, Institute for Genome Research, University of Tokushima, Tokushima 770-8503, Japan
[3]Department of Microbiology, Hyogo College of Medicine, Nishinomiya 663-8501, Japan

Correspondence to: I. Kawamura, E-mail: ikuo_kawamura@mb.med.kyoto-u.ac.jp

Received 16 April 2010, *accepted* 1 October 2010

Abstract

A major concern still prevails as to the reason why various mycobacteria are able to persist within infected host in which protective immunity is generated. To address this question, we monitored the generation of protective T cells during infection with *Mycobacterium bovis* bacillus Calmette-Guérin (BCG). $CD4^+$ T cells obtained 3 weeks after infection conferred protection against *Mycobacterium tuberculosis* challenge and produced IFN-γ and tumor necrosis factor (TNF)-α upon antigen stimulation. However, these abilities were decreased after 6 weeks of infection even though BCG was not thoroughly eliminated from the host. We analyzed the expression of ligands for the CD28/CTLA-4 family receptors on antigen-presenting cells and found that the expression of PD-L1, a ligand for programmed cell death-1 (PD-1), was up-regulated later than 3 weeks of infection. We also found that bacterial numbers in the spleen of PD-1-deficient mice were significantly reduced compared with wild-type mice at 6 and 12 weeks after BCG infection. Furthermore, $CD4^+$ T cells of PD-1-deficient mice showed a higher ability to confer protection and produce IFN-γ and TNF-α even at 12 weeks after infection. These results indicate that the PD-1–PD-L1 pathway impairs T_h1 immunity in the late stage of BCG infection, thereby facilitating the bacterial persistence in the host.

Keywords: Mycobacterium, PD-1, persistent infection, T_h1 immunity

Introduction

Tuberculosis (TB) caused by *M. tuberculosis* (Mtb) is one of the leading threats for humans (1). One-third of the world's population is exposed to Mtb and ~10% of individuals exposed develop TB. Although most of the remaining people do not suffer from disease during their lifetime, TB eventually emerges in those whose immune system is compromised by aging, HIV infection or malnutrition (2, 3). *Mycobacterium bovis* bacillus Calmette-Guérin (BCG), an attenuated vaccine strain, could also persist in the host body for a long time and occasionally causes disease in acquired immunodeficiency syndrome patients even after several decades of vaccination (4–6). These indicate that Mtb and BCG are capable of surviving in the host in which protective immunity is generated. Therefore, an understanding of the mechanisms by which these mycobacteria evade the host defense system is important for the development of effective therapies and the rational design of novel vaccines.

Protective immunity to mycobacteria is mediated by T_h1-type $CD4^+$ T cells with the aid of other types of T cells (7–11). T_h1 cells produce IFN-γ and tumor necrosis factor (TNF)-α in response to mycobacterial antigens, which are critical for macrophage activation and control of bacterial replication (12). Cell-to-cell contact between T cells and antigen-presenting cells (APC) is an important event for induction of the T-cell-mediated immune response. Indeed, the interaction of co-stimulatory and co-inhibitory receptors (e.g. CD28 and CTLA-4) expressed on T cells with the ligands (e.g. B7-1 and B7-2) on APC influences the magnitude and duration of antigen-specific T-cell response (13). Programmed cell death 1 (PD-1, also known as CD279) is a new member of the CD28/CTLA-4 receptor family, which was originally identified in a T-cell hybridoma undergoing apoptotic cell death (14). PD-1 expression is induced on activated T cells and B cells (15), and its constitutive

expression on $CD4^+$ T cells is observed during immunosenescence (16). PD-1 has two ligands, PD-L1 (B7-H1 or CD274) and PD-L2 (B7-DC or CD273). PD-L2 expression is restricted to activated dendritic cells (DC) and macrophages, whereas PD-L1 is constitutively expressed on a wide variety of cells (17). Furthermore, PD-L1 expression on cells including APC is up-regulated after stimulation with IFN-γ and toll-like receptor ligands (18–20). Interaction of PD-1 with the ligands provides an inhibitory signal that regulates T-cell activation to induce and maintain peripheral tolerance (21).

Recent studies have shown that pathogenic microbes exploit the PD-1–PD-L pathway as a strategy for immune evasion and persistent infection (22). For example, PD-1 is highly expressed on functionally impaired (exhausted) T cells in a chronic infection with lymphocytic choriomeningitis virus (LCMV). Blockade of the PD-1–PD-L1 pathway restores T-cell function and promotes clearance of the persisting virus (23). During infection with HIV, hepatitis B virus and hepatitis C virus, T-cell exhaustion and disease progression are associated with up-regulation of PD-1 on antigen-specific T cells (24–26). In addition to chronic viral infection, *Helicobacter pylori* suppresses the T-cell response by up-regulating PD-L1 expression on gastric epithelial cells that are thought to act as APC. *In vitro* blockade of the PD-1 signaling enhances cytokine production and proliferation by T cells on antigen stimulation (27), suggesting that the PD-1–PD-L pathway may also play a role in persistent infection with bacteria.

In mycobacterial infection, $CD4^+$ T cells isolated in the initial stage of infection exert strong cytokine production and proliferation, but these responses are diminished in the late stage of infection (28–30). These findings raised the possibility that the antigen-specific T-cell response is impaired or modulated by some inhibitory mechanism, allowing mycobacteria to achieve persistent infection. In this study, we investigated whether the PD-1–PD-L pathway contributes to the inhibition of T_h1 immune response to BCG. Our results clearly show that although protective T cells were generated by 3 weeks after BCG infection, T-cell responses were impaired in the later period by the PD-1–PD-L1 co-inhibitory pathway.

Methods

Antibodies

The monoclonal antibodies specific for mouse B7-1 (16-10A1), B7-2 (GL1), CD4 (GK1.5), CD11c (N418), CD44 (IM7), CD62L (MEL-14), F4/80 (BM8), herpes virus entry mediator (HVEM, LH1), ICOS ligand (ICOS-L, IHK5.3), PD-1 (RMP1-30), PD-L1 (MIH5) or PD-L2 (TY25) and isotype control antibodies were purchased from eBioscience (San Diego, CA, USA). The antibody to CD16/CD32 (2.4G2), $I\text{-}A^b$ (M5/114.15.2), IFN-γ (XMG1.2) and TNF-α (MP6-XT22) were purchased from BD Biosciences (San Jose, CA, USA).

Mice

C57BL/6 mice were purchased from Japan SLC (Shizuoka, Japan). PD-1-deficient ($PD\text{-}1^{-/-}$) mice on a C57BL/6 background were kindly provided by Dr Tasuku Honjo (Kyoto University) and maintained under specific pathogen-free conditions. All mice used in the experiments were 8–10 weeks old. All the animal experimental procedures were approved by the Animal Ethics and Research Committee of Kyoto University Graduate School of Medicine, Japan.

Bacteria

Mycobacterium bovis BCG strain Pasteur and Mtb strain H37Rv were grown at 37°C to mid-log phase in Middlebrook 7H9 broth (BD Bioscience) supplemented with 0.2% glycerol and albumin dextrose catalase (ADC) enrichment consisting of 0.5% albumin, 0.2% dextrose and 3 μg ml^{-1} catalase. Bacteria were harvested, stirred vigorously with glass beads (3 mm in diameter) to disperse the bacterial clumps and left to stand for 30 min. The upper part of the suspension, without visible clumps, was collected and stored at −80°C in aliquots. After thawing, the bacterial suspension was centrifuged at 150 × *g* for 2 min to remove any clumps, and only the upper part of the suspension was used for the experiments. Bacterial numbers in the preparation were determined by counting the colonies after plating the diluted suspension on Middlebrook 7H10 agar (BD Bioscience) plates supplemented with ADC enrichment, 0.2% glycerol and 50 μg ml^{-1} oleic acid. The plates were incubated at 37°C and the colony-forming units (CFU) were counted after 3 weeks. The absence of bacterial clumps was confirmed using the LIVE/DEAD BacLight Bacterial Viability kit (Invitrogen, Carlsbad, CA, USA).

Infection and adoptive cell transfer

Mice were infected intravenously (i.v.) with 10^6 CFU of BCG. The spleen and lung were recovered and homogenized in PBS at the indicated time points after infection. The serially diluted homogenates were plated onto 7H10 agar plates and bacterial number was enumerated. In some experiments, spleens were removed at the indicated times after infection and single-cell suspensions were prepared through a 70-μm nylon cell strainer (BD Biosciences) using a 2.5-ml syringe plunger. After RBC lysis with NH_4Cl/Tris solution, $CD4^+$ and $CD8^+$ T cells were isolated at >95% purity using the BD IMag Mouse CD4 T Lymphocyte enrichment set and the CD8 T Lymphocyte enrichment set (both from BD Bioscience), respectively. Purified T cells (5×10^6 cells) were injected i.v. into naive WT mice. Mice were infected i.v. with 10^5 CFU of Mtb 1 h after cell transfer. Ten days after Mtb infection, the spleen and lung were homogenized and the number of CFU in the organs was determined.

Analysis of antigen-specific T-cell response

Mice were infected i.v. with BCG and $CD4^+$ T cells were purified from the spleen at 1, 3, 6 and 12 weeks after infection. Bone marrow-derived DC (BMDC) were prepared as described previously (31). In brief, bone marrow cells were removed from the femurs and tibias of WT mice and cultured in RPMI 1640 supplemented with 2 mM glutamine, 10% FCS, 100 U ml^{-1} penicillin, 100 μg ml^{-1} streptomycin and 20 ng ml^{-1} granulocyte macrophage colony-stimulating factor (R&D Systems, Minneapolis, MN, USA). On days 3 and 6, the culture medium was replenished and cells were used on days 7–8 of culture. To prepare BCG-pulsed APC, BMDC were infected with BCG (multiplicity of infection = 5) for 16 h and treated with mitomycin C (50 μg ml^{-1}; Nacalai Tesque,

Kyoto, Japan) for 30 min at 37°C. $CD4^+$ T cells (1×10^6 cells ml^{-1}), obtained from naive and BCG-infected mice, were stimulated with BCG-pulsed BMDC (5×10^5 cells ml^{-1}) for 60 h. Cell proliferation was determined by labeling of cultures for the last 12 h with 5-bromo-2-deoxyuridine using the Cell Proliferation ELISA kit (Roche Diagnostics, Mannheim, Germany). In addition, the culture supernatants were harvested after 48 h of culture and the concentration of cytokines was measured using the BD CBA Mouse Inflammation kit for IFN-γ, IL-10 or TNF-α (BD Biosciences) and the ELISA kit for transforming growth factor (TGF)-β1 (eBioscience). In some experiments, spleen cells (10^6 cells per well) of naive and BCG-infected mice were plated in round-bottom 96-well plates and stimulated with purified-protein derivatives (PPD) (5 μg ml^{-1}; Japan BCG, Kiyose, Japan) for 6 h. Brefeldin A (50 μg ml^{-1}; BD Biosciences) was added 2 h after PPD stimulation. Cells were treated with PE-Cy5-conjugated anti-CD4 antibody for 20 min on ice, followed by fixation for 30 min in 4% PFA solution. Intracellular IFN-γ and TNF-α were stained using the Cytofix/Cytoperm kit (BD Biosciences) according to the manufacturer's instructions and analyzed by flow cytometry.

Flow cytometry

Spleens were recovered from BCG-infected WT mice at the indicated time points and single-cell suspensions were prepared as described above. Cells were incubated with anti-CD16/CD32 antibody for 10 min to block Fc binding and treated with FITC-conjugated anti-I-A^b antibody and PE-conjugated antibody to B7-1, B7-2, HVEM, ICOS-L, PD-L1, PD-L2 or the isotype control antibody for 20 min on ice. In some experiments, cells were stained with PE-Cy5-conjugated anti-CD4 antibody, FITC-conjugated anti-CD44 antibody and PE-conjugated antibody to CD62L or PD-1 for 20 min on ice. To determine apoptosis of memory $CD4^+$ T cells, splenocytes were collected from BCG-infected WT and PD-$1^{-/-}$ mice and treated with PE-Cy5-conjugated anti-CD4 antibody and FITC-conjugated anti-CD44 antibody, followed by staining with Annexin V-PE (Calbiochem, San Diego, CA, USA). Intracellular Foxp3 staining for $CD4^+$ T cells was performed using the FITC anti-Foxp3 staining kit (eBioscience) according to the manufacturer's recommendations. All stained cells were analyzed on a FACSCalibur using CELLQuest software (BD Biosciences) or FlowJo software (Tree Star, Inc., Ashland, OR, USA).

Statistical analysis

For comparisons between two groups, the Student's *t*-test was used when the variances of the groups were judged to be equal by the *F*-test. Multigroup comparisons of mean values were made according to the analysis of variance and the Fisher's protected least significant difference *post hoc* test after the confirmation of homogeneity of the variances among the groups had been confirmed using the Bartlett's test. Statistical significance was determined as $P < 0.05$.

Results

T-cell-mediated protective immunity is attenuated in the late stage of BCG infection

To determine the course of BCG infection, we infected wild-type (WT) C57BL/6 mice i.v. with BCG and monitored the bacterial numbers in the spleen and lung. As shown in Fig. 1A, BCG replicated in these organs within a week after infection. Thereafter, the bacterial number gradually decreased in a time-dependent manner. However, a significant number of bacteria still remained in both organs at 12 weeks after infection.

Because $CD4^+$ T cells play an essential role in protection against mycobacterial infection (7–11), we investigated the generation of protective T cells by an adoptive cell transfer

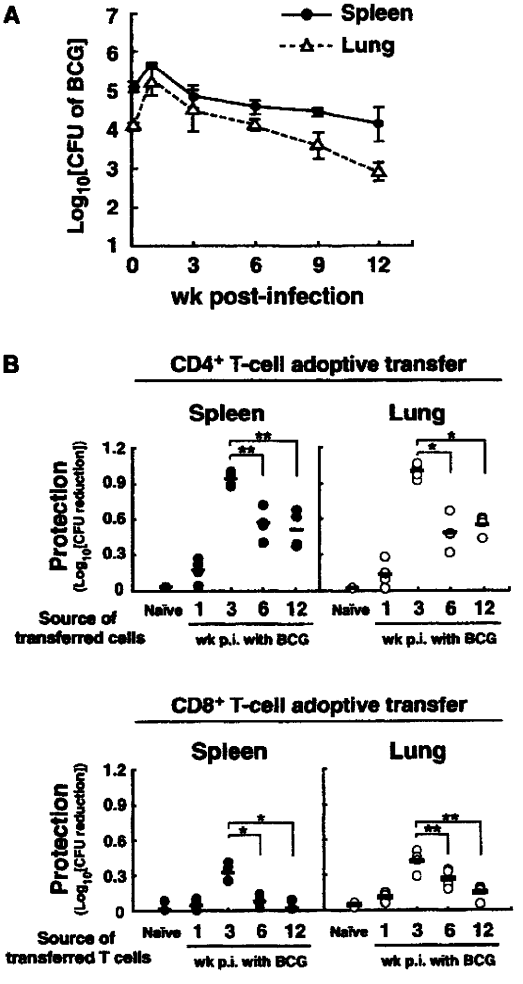

Fig. 1. Kinetics of the bacterial numbers in organs after BCG infection and the protective efficacy of T cells obtained from BCG-infected mice against Mtb infection. (A) WT mice were infected i.v. with 10^6 CFU of BCG. Bacterial numbers in the spleens and lungs were determined. Data represent the means ± SD of CFU in five mice at each time point. (B) $CD4^+$ and $CD8^+$ T cells were purified from spleens at the indicated weeks post-infection (wk p.i.) with BCG and transferred into naïve WT mice. Mice were infected with 10^5 CFU of Mtb 1 h after T-cell transfer. Ten days after Mtb infection, the numbers of bacteria in the spleens and lungs were determined. Each symbol represents a reduction of CFU in the experimental groups compared with that in non-transferred group. Horizontal bars indicate the mean values for each group. $*P < 0.01$, $**P < 0.05$. Results are representative of three independent experiments.

experiment. Naive WT mice were transferred with $CD4^+$ T cells from the spleens of BCG-infected mice and subsequently infected i.v. with Mtb. Ten days later, the bacterial numbers in the spleen and lung were determined. Mice transferred with $CD4^+$ T cells obtained at 1 week after infection with BCG hardly exhibited protection against a challenge infection with Mtb. On the other hand, $CD4^+$ T cells obtained at 3, 6 and 12 weeks after BCG infection conferred protection on recipient mice (Fig. 1B). However, the ability of T cells obtained at 6 and 12 weeks after infection was significantly reduced compared with T cells obtained at 3 weeks after infection, even when BCG could still be detected in the donors (Fig. 1A). These results suggested that although $CD4^+$ T-cells-mediating protective immunity were generated as early as 3 weeks after infection, the protective efficacy was decreased in the later stages. This result may explain why BCG is not easily eradicated from the host.

In addition to $CD4^+$ T cells, it has been shown that $CD8^+$ T cells also play a role in protection against Mtb (7, 8, 32, 33). Thus, we investigated the efficacy of $CD8^+$ T cells from BCG-infected mice on induction of protective immunity by the adoptive cell transfer experiment. Similar to $CD4^+$ T cells, protective $CD8^+$ T cells were generated at 3 weeks after infection (Fig. 1B). However, the protective effect was markedly weaker than that of $CD4^+$ T cells and was mostly decreased to the marginal levels by 12 weeks after infection. In the following experiments, therefore, we examined the mechanism by which $CD4^+$ T-cell functions were decreased during BCG infection.

Antigen-specific $CD4^+$ T-cell response is impaired in the late stage of BCG infection

To clarify whether the reduction of protective efficacy in the late stage of infection is due to the functional impairment of $CD4^+$ T cells, we investigated the ability of $CD4^+$ T cells to produce IFN-γ and TNF-α and assessed their proliferation upon stimulation with BCG-pulsed BMDC. $CD4^+$ T cells obtained at 1 week after infection did not produce IFN-γ or TNF-α and did not exhibit a significant proliferative response (Fig. 2A). On the other hand, T cells obtained at 3 weeks after infection produced a large amount of cytokines and exhibited a significant proliferative response. However, the responses of $CD4^+$ T cells obtained at 6 and 12 weeks after infection were significantly weaker than those of T cells obtained at 3 weeks after infection.

Recently, it has been reported that T cells producing both IFN-γ and TNF-α mediate protection against parasitic and viral infections (34–36). Therefore, the possibility exists that T cells producing both these cytokines may contribute to protection against Mtb infection. We analyzed the profile of cytokine production in $CD4^+$ T cells and determined the kinetics of the T-cell population during the course of BCG infection. As shown in Fig. 2B, $CD4^+$ T cells producing both IFN-γ and TNF-α were virtually undetectable in spleen cells at 1 week after infection but were generated at 3 weeks. However, the number of T-cell populations was markedly reduced at 6 weeks and remained at a low level until 12 weeks after infection. These results showed that protection against Mtb correlates with the generation of the $CD4^+$ T-cell population, suggesting that T cells capable of producing both IFN-γ and TNF-α mediate protective immunity. It is likely that a decrease in protective immunity in the late stage of BCG infection is, at least in part, caused by a reduction of the $CD4^+$ T-cell populations.

It has been shown that $CD4^+$ $CD25^+$ $Foxp3^+$ regulatory T (Treg) cells and IL-10-producing $CD4^+$ T (Tr1) cells are increased during Mtb infection and contribute to suppression of host immune responses (37–40). We investigated whether the number of Treg cells or Tr1 cells is increased in the late stage of BCG infection. First, spleen cells were collected from BCG-infected mice and the population of Treg cells was analyzed by flow cytometry. We found 9.58 ± 1.4% of $CD25^+$ $Foxp3^+$ cells in the naive $CD4^+$ T-cell population and the T-cell population did not increase during BCG infection (Fig. 3A). We next evaluated the generation of IL-10-producing Tr1 cells after BCG infection. However, no significant increase in IL-10 production was observed in $CD4^+$ T cells at 6 or 12 weeks after infection (Fig. 3B). These results suggested that Treg cells and Tr1 cells do not contribute to the impairment of T_h1 response, which was observed later than 6 weeks of BCG infection.

PD-L1 expression on APC is up-regulated in the late stage of BCG infection

It has been shown that the antigen-specific T-cell response is regulated by a sum of co-stimulatory and co-inhibitory signals that are transduced to T cells through the interaction between the CD28/CTLA-4 family receptors expressed on T cells and the ligands expressed on APC (13). We investigated whether these signals are involved in the functional impairment of $CD4^+$ T cells during BCG infection by measuring the expression of ligands for the CD28/CTLA-4 family receptors on MHC class II^{high} ($I\text{-}A^{high}$) APC including DC and macrophages (Fig. 4A). The expression levels of B7-1 (CD80) and B7-2 (CD86) were elevated at 3 weeks after infection and gradually decreased to a level similar to those of uninfected APC at 12 weeks. Because B7 molecules contribute to the control of chronic Mtb infection (41), a decrease in their expression may contribute to the impairment of T-cell response in the late stage of BCG infection. The expression of ICOS-L did not change in the course of BCG infection. On the other hand, a cell population positive for HVEM [a ligand for B and T lymphocyte attenuator (BTLA)] (42) temporarily appeared at 3 weeks and disappeared at 6 weeks after infection. Importantly, the expression of PD-L1 was up-regulated on APC at 3 weeks and the expression level remained higher than that of uninfected APC until 12 weeks after infection. However, the expression of PD-L2 was not induced by BCG infection. We also observed similar patterns of their expressions in DCs ($CD11c^{high}$ cells) and macrophages ($F4/80^+$ cells), respectively (data not shown). These results indicated that PD-L1, as compared with other ligands for the CD28/CTLA-4 family receptors, is predominantly expressed and maintained on APC even at the late stage of infection. To know if the PD-1, the counterpart receptor for PD-L1, is also expressed or not, we looked at the PD-1 expression on $CD4^+$ T cells. As expected, the increase in the PD-1 expression on $CD4^+$ T cells was observed 3 weeks after infection and maintained until 12 weeks (Fig. 4B). The expression of PD-1 was detected preferentially in $CD44^{high}$

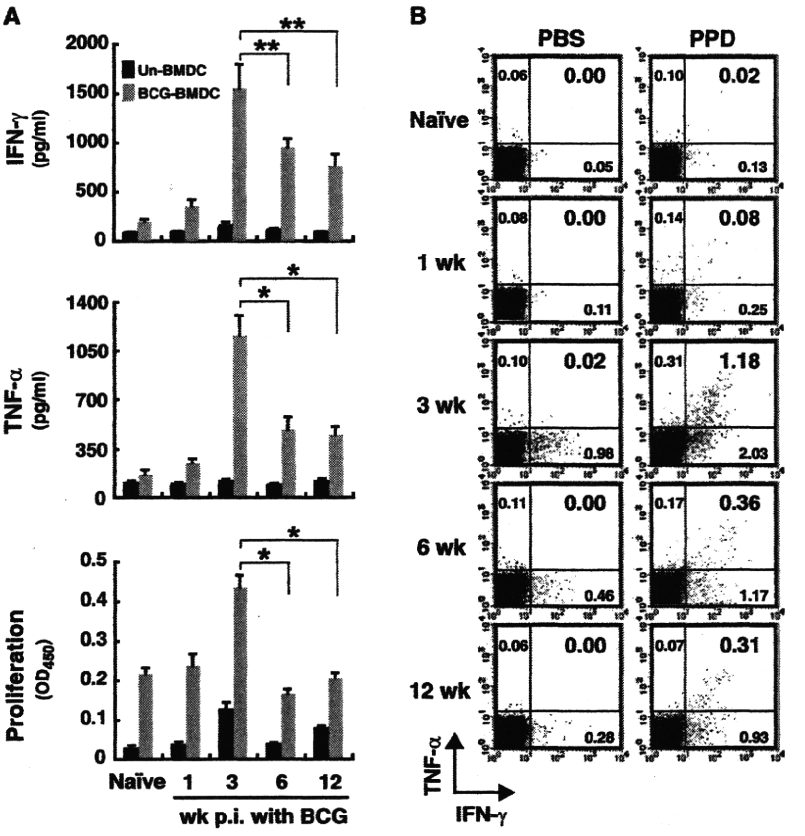

Fig. 2. Antigen-specific responses of CD4$^+$ T cells obtained from BCG-infected mice. (A) CD4$^+$ T cells were isolated from spleens at the indicated weeks post-infection (wk p.i.) with BCG and cultured with unpulsed BMDC (black bars) or BCG-pulsed BMDC (gray bars) for 48 h. The culture supernatants were harvested and the concentration of cytokines was measured. T-cell proliferation was measured by 5-bromo-2-deoxyuridine incorporation. Data are the means ± SD of triplicate cultures. *$P < 0.01$, **$P < 0.05$. (B) Splenocytes were isolated from BCG-infected mice at the indicated times after BCG infection. Cells were stimulated with PPD for 6 h and intracellular IFN-γ and TNF-α were analyzed by flow cytometry. Each value indicates the percentage of cells producing both IFN-γ and TNF-α in CD4$^+$ lymphocytes. Results are representative of four independent experiments.

CD4$^+$ T cells but not in CD44^{low} CD4$^+$ T cells, indicating that PD-1 was exclusively expressed in memory T-cell population (Fig. 4B). These results suggested a possible involvement of PD-1–PD-L1 pathway in the reduction of protective ability of CD4$^+$ T cells after BCG infection.

CD4$^+$ T-cell-mediated protection in PD-1$^{-/-}$ mice is maintained in the late stage of BCG infection

To confirm whether the PD-1–PD-L1 pathway is involved in the reduction of host protective immunity, WT and PD-1$^{-/-}$ mice were infected with BCG and the kinetics of bacterial number was determined. No difference was detected in the number of CFU in the spleens of WT and PD-1$^{-/-}$ mice until 3 weeks after infection (Fig. 5A). However, at 6 and 12 weeks after infection, the number of CFU in PD-1$^{-/-}$ mice was significantly reduced compared with WT mice. We then performed an adoptive cell transfer experiment to compare the ability of CD4$^+$ T cells from WT and PD-1$^{-/-}$ mice to confer protection against challenge infection with Mtb. CD4$^+$ T cells obtained from the spleen of both WT and PD-1$^{-/-}$ mice at 3 weeks after infection conferred a similar level of protection against Mtb in the spleen and lung of recipient mice. However, consistent with the data presented above, the protective ability of WT T cells obtained at 6 and 12 weeks after infection was reduced (Fig. 5B). The ability of PD-1$^{-/-}$ T cells was also reduced at 6 and 12 weeks but was significantly higher than that of WT T cells.

PD-1–PD-L1 pathway is involved in the impairment of CD4$^+$ T-cell response in the late stage of BCG infection

To verify that the PD-1–PD-L1 pathway modulates the immune response of antigen-specific CD4$^+$ T cells generated after BCG infection, we compared the ability of WT and PD-1$^{-/-}$ CD4$^+$ T cells to produce IFN-γ and TNF-α, and also analyzed the proliferative responses upon stimulation with BCG-pulsed BMDC. No difference was found in the production of IFN-γ and TNF-α between WT and PD-1$^{-/-}$ CD4$^+$ T cells obtained at 3 weeks after infection (Fig. 6A). However, CD4$^+$ T cells obtained from PD-1$^{-/-}$ mice at 6 and 12 weeks after infection produced a significantly higher level

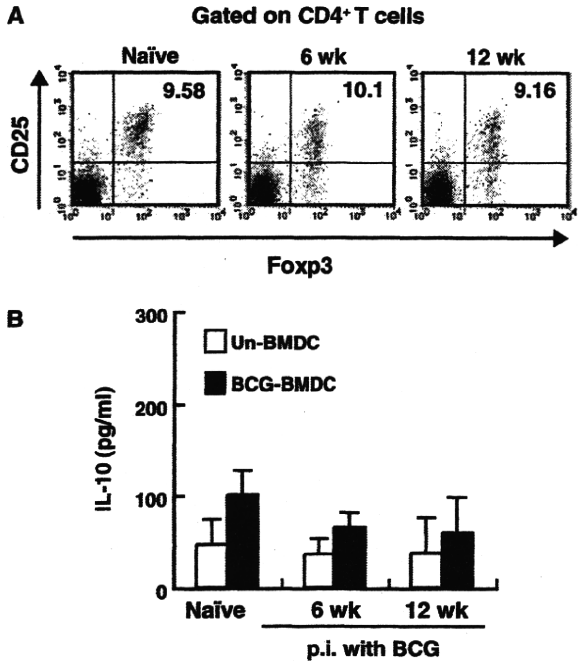

Fig. 3. Analysis of Treg cells and IL-10-producing CD4$^+$ T cells after BCG infection. (A) WT mice were infected with BCG and the frequency of CD4$^+$ CD25$^+$ Foxp3$^+$ T cells in spleens was determined at the indicated times after BCG infection. Numbers indicate the percentage of Treg cells. (B) CD4$^+$ T cells were isolated at the indicated weeks post-infection (wk p.i.) and stimulated with unpulsed BMDC (open bars) or BCG-pulsed BMDC (filled bars) for 48 h. IL-10 concentration in the culture supernatants was determined by using a cytometric bead array kit. Data represent the means ± SD of triplicate cultures. Results are representative of three independent experiments.

of cytokines compared with WT T cells. Similarly, PD-1$^{-/-}$ T cells obtained in the late stage of infection exhibited a higher proliferative response.

We next compared the generation of CD4$^+$ T cells capable of producing both IFN-γ and TNF-α between WT and PD-1$^{-/-}$ mice after BCG infection. Both groups of mice generated a similar level of the CD4$^+$ T-cell population at 3 weeks after infection. The frequency of T cells in PD-1$^{-/-}$ mice was maintained at a higher level at 6 and 12 weeks after infection, while the T-cell population of WT mice was reduced after 6 weeks of infection (Fig. 6B). Consistent with the kinetics of cytokine-producing T cells, the frequency of memory CD4$^+$ T cells (CD44^{high} CD62L^{low} CD4$^+$ T cells) was also maintained at the high level in PD-1$^{-/-}$ mice compared with WT mice (45.4% versus 29.1% and 35.7% versus 23.8% at 6 and 12 weeks, respectively) in the late stage of infection (Fig. 6C). In order to determine whether the reduction of memory CD4$^+$ T-cell population in WT mice was due to programmed cell death or not, we compared the levels of cell death of memory CD4$^+$ T cells (CD44^{high} CD4$^+$ T cells) between WT and PD-1$^{-/-}$ mice by Annexin V staining assay. As shown in Fig. 6D, a similar level of apoptosis was detected in the memory T-cell populations of WT and PD-1$^{-/-}$ mice at 6 and 12 weeks after BCG infection. This finding suggested that the PD-1-dependent difference is ascribed to the functional reduction of memory T cells, not to the apoptotic cell death of memory T cells in the late stage of BCG infection. Taken together, these results may account in part for the fact that CD4$^+$ T cells of PD-1$^{-/-}$ mice confer more effective protection compared with WT T cells (Fig. 5B).

Discussion

On infection with Mtb or BCG, protective T cells are generated in the infected host. However, T-cell-mediated immunity does not easily eradicate these mycobacteria because they have evolved effective strategies to overcome host defense mechanisms (43). Recent studies have identified various virulence-associated genes and intracellular survival mechanisms of mycobacteria (44–46). However, the entire survival strategy remains uncertain. The recent emergence of multidrug-resistant Mtb strains highlights the need for research to unravel the mechanisms that enable this bacterium to be successfully parasitic in humans.

Several studies have demonstrated that the PD-1-signaling pathway is activated during persistent infection with various microorganisms and contributes to impairment of protective immunity. A recent study showed that *in vitro* blockade of PD-1 signaling with the specific antibody enhanced IFN-γ production by T cells of TB patients on stimulation with Mtb antigen (47), indicating that this inhibitory pathway also affects the T-cell function during mycobacterial infection. In the present study, we demonstrated that the PD-1 signaling is actually involved in the impairment of T_h1 response during BCG infection *in vivo*. We found that the ability of WT CD4$^+$ T cells to mediate protection and produce T_h1 cytokines was reduced after 6 weeks of BCG infection. However, the ability was maintained in PD-1$^{-/-}$ CD4$^+$ T cells compared with WT T cells in the late stage of infection. Consistent with the functional impairment of CD4$^+$ T cells observed later than 6 weeks after BCG infection, PD-1 expression was induced in the memory CD4$^+$ T cells and maintained even after 6 weeks. Moreover, PD-L1, as compared with other ligands for the CD28/CTLA-4 family receptors, was dominantly expressed on APC at the late stage of infection. Based on these findings, we concluded that the interaction transduces an inhibitory signal to effector T-cells-mediating protection, resulting in the impairment of T-cell responses required for protective immunity.

We investigated here the effect of PD-1 signal pathway on the effector functions of CD4$^+$ T cells generated in mice infected with BCG because CD4$^+$ T cells played a crucial role in protection compared with CD8$^+$ T cells (8–11). A reason for the lower contribution of CD8$^+$ T cells may be an inferior ability of BCG to induce antigen-specific CD8$^+$ T cells (48–50). On the other hand, several studies have shown that the enhanced expression of PD-1 on antigen-specific CD8$^+$ T cells is associated with their functional exhaustion during chronic viral infection (23–26). As Mtb infection induces a strong CD8$^+$ T-cell response in the infected host, therefore, it will be important to analyze the effect of PD-1 signaling on the function of both CD4$^+$ and CD8$^+$ T-cell populations in Mtb infection. We are currently investigating the role of PD-1

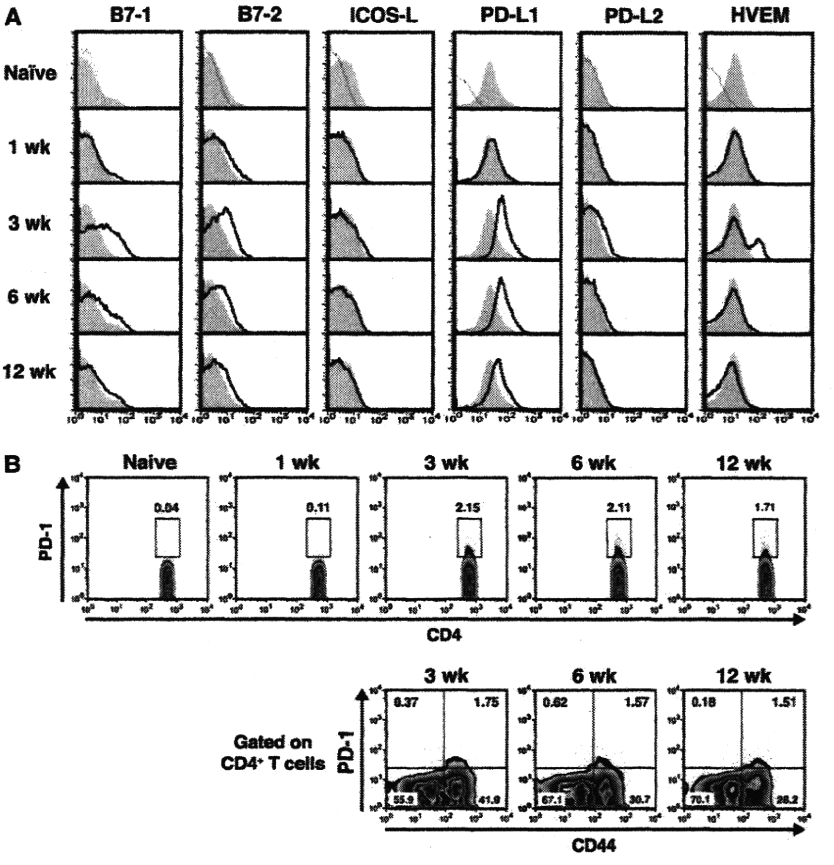

Fig. 4. Kinetics of the expression of co-stimulatory and co-inhibitory molecules on APC and PD-1 on $CD4^+$ T cells after BCG infection. Splenocytes were prepared from BCG-infected mice at the indicated times after infection. (A) Expression level of each molecule on APC ($I\text{-}A^{high}$ cells) was analyzed by flow cytometry. Shaded histograms, naïve cells; solid lines, BCG-infected cells; dotted lines, isotype controls. (B) Splenocytes were collected from WT mice after BCG infection and the kinetics of PD-1 expression on $CD4^+$ T cells was measured by flow cytometry (upper panels). Alternatively, the expression of PD-1 on memory $CD4^+$ T cells was determined on $CD44^{high}$ $CD4^+$ T cells (lower panels). Numbers indicate the percentage of $CD4^+$ T cells in each area. Results are the representative of four independent experiments.

signal pathway in the function of antigen-specific T cells generated by Mtb infection.

The expression of PD-1 was induced in memory $CD4^+$ T cells after 3 weeks of BCG infection, at which stage the protective T cells were generated. Since T-cell receptor-mediated signaling induces PD-1 expression of T cells (15, 17), it appears that the expression was observed concurrently with generation of IFN-γ and TNF-α-producing $CD4^+$ T cells after BCG infection. Similar to the PD-1 expression, PD-L1 expression on APC was enhanced later than 3 weeks after infection. PD-L1 is constitutively expressed on a variety of tissues and cells, and the expression is enhanced by IFN-γ (18, 20). Furthermore, the up-regulation of PD-1 expression on macropahges is shown to be mediated by T_h1 cells (19). From these findings, it seems likely that the up-regulation of PD-L1 is induced by IFN-γ produced from $CD4^+$ T cells that was generated after BCG infection. It is noteworthy that APC at 3 weeks after infection highly expressed not only PD-L1 but also B7 molecules that contribute to control of Mtb growth at the chronic stage of infection (41). It has been shown that PD-1-mediated inhibitory signals can be overcome by co-stimulatory signals through CD28 (51). Therefore, it is possible that the inhibitory signals might be canceled by an interaction of B7 molecules with CD28 at 3 weeks after BCG infection. In the later stage of infection, however, the PD-1-mediated signal might become dominant because of a decrease in the expression of B7 molecules and eventually interfere with protective immunity, allowing the bacteria to infect persistently.

As shown in Fig. 5B, the numbers of CFU in the spleen of $PD\text{-}1^{-/-}$ mice were significantly decreased at 6 and 12 weeks after infection compared with WT mice. However, no difference was found in the bacterial numbers in the lung between WT and $PD\text{-}1^{-/-}$ mice (data not shown). Our preliminary experiments revealed that BCG did not enhance PD-L1 expression on APC in the lung even when the expression on APC in the spleen was up-regulated by infection. This result suggested that activation of the PD-1–PD-L1 pathway is induced by systemic infection with BCG in the spleen but not in the lung. Therefore, the difference in PD-L1 expression

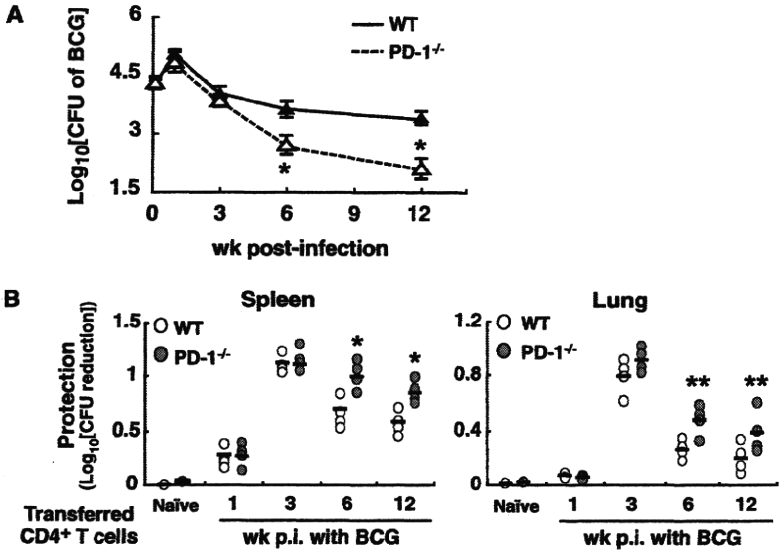

Fig. 5. Comparison of protective immunity to BCG between WT and PD-1$^{-/-}$ mice. (A) WT and PD-1$^{-/-}$ mice were infected with 10^6 CFU of BCG. Bacterial numbers in spleens were evaluated at the indicated time points. Data are the mean ± SD of CFU from four mice per each time point. (B) After BCG infection, CD4$^+$ T cells were purified from the spleens of WT or PD-1$^{-/-}$ mice and transferred into WT recipient mice. Mice were infected with 10^5 CFU of Mtb, and bacterial numbers in the spleen and lung were determined after 10 days. Data are expressed as described in Fig. 1B. $^*P < 0.01$, $^{**}P < 0.05$ as compared with WT mice. Results are representative of two independent experiments.

appears to account for the observed difference in bacterial clearance between the spleen and the lung of infected mice. In addition, we found that the expression of PD-Ls was up-regulated on APC in both the lung and the spleen as early as 10 days after Mtb infection (data not shown), suggesting that the inability of BCG to induce PD-L1 expression in the lung might be because of the attenuated virulence or immunogenicity of BCG (52, 53).

Because Treg cells and Tr1 cells are implicated in the suppression of immune response to Mtb (37–40), we investigated whether that these T cells contribute to the reduction of T_h1 response during BCG infection. However, we did not observe a significant increase in the population of Treg cells or IL-10-producing Tr1 cells in the late stage of infection. Previous studies have shown that *in vivo* depletion of Treg cells does not affect protective immunity to BCG (37). Furthermore, bacterial clearance has been observed similarly in C57BL/6 WT and IL-10$^{-/-}$ mice infected with BCG (54, 55). Therefore, it appears that Treg cells and Tr1 cells do not play a major role in the impairment of T-cell-mediated immunity in the late stage of BCG infection. In addition, TGF-β1-producing CD4$^+$ T (T_h3) cells have been postulated to suppress the immune response to Mtb infection (56). However, we were unable to detect a significant increase in TGF-β1 production by CD4$^+$ T cells in the late stage of BCG infection (data not shown).

CD4$^+$ T cells capable of producing both IFN-γ and TNF-α were generated by 3 weeks after infection with BCG. These cytokines are essential for the control of Mtb infection (12). The appearance of cytokine-producing CD4$^+$ T cells strongly correlated with the magnitude of protection because protective efficacy and the frequency of CD4$^+$ T cells producing IFN-γ and TNF-α peaked at 3 weeks after infection and were simultaneously decreased thereafter in WT mice. Consistent with our results, recent studies have shown that the appearance of T cells producing both IFN-γ and TNF-α correlates with protection against infection with various pathogens including Mtb (34–36, 57). Unlike WT mice, however, the T-cell population of PD-1$^{-/-}$ mice was maintained even in the late stage of infection. CD4$^+$ T cells capable of producing both IFN-γ and TNF-α may therefore play an important role in protective immunity to BCG, and the PD-1-dependent signal may be associated with the decrease in the T-cell population.

It has been shown that the number of antigen-specific CD4$^+$ T cells is reduced as a result of a contraction of memory CD4$^+$ T cells after the antigen or pathogen was eliminated from the host (58, 59). In this study, however, we observed the functional reduction of protective CD4$^+$ T cells even when BCG was still detectable in the host. As there was no difference in the level of apoptosis of memory CD4$^+$ T cells between WT and PD-1$^{-/-}$ mice, it is clear that the reduction is not a reflection of cell death. It is therefore assumed that the PD-1-dependent reduction of effector T cells is due to the result of a mechanism distinct from that of the conventional contraction of antigen-specific T cells.

Our study showed that the PD-1–PD-L1 pathway contributes to the impairment of protective immunity in the late stage of BCG infection. In other words, blockade of the co-inhibitory pathway appears to be a useful strategy for therapy of latent TB and enhancement of vaccination efficacy. In fact, during chronic infection with LCMV and simian immunodeficiency virus, treatment with anti-PD-1 antibody resulted in the rapid expansion of virus-specific T cells and

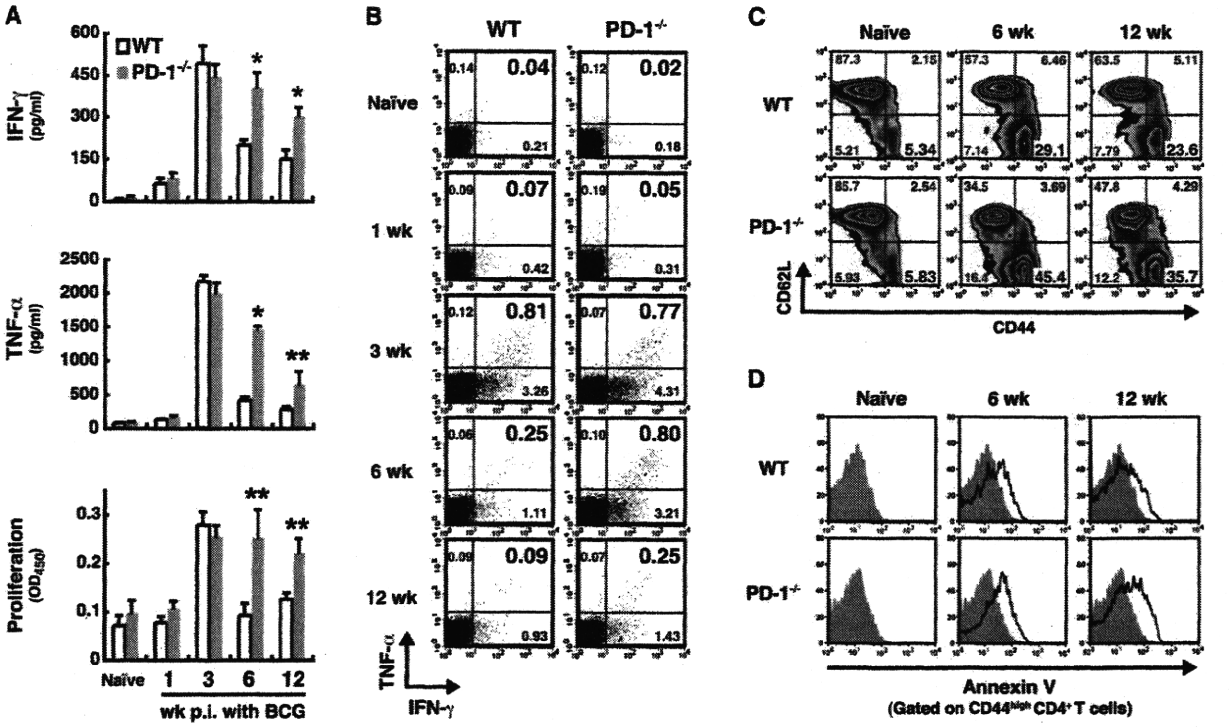

Fig. 6. Functional and phenotypic differences of CD4$^+$ T cells obtained from WT and PD-1$^{-/-}$ mice after BCG infection. (A) CD4$^+$ T cells were purified from WT and PD-1$^{-/-}$ mice after BCG infection and cultured with BCG-pulsed BMDC. IFN-γ and TNF-α production and proliferation of CD4$^+$ T cells were measured. Data are the means ± SD of triplicate cultures. *$P < 0.01$, **$P < 0.05$ as compared with WT mice. (B) Splenocytes were isolated from WT and PD-1$^{-/-}$ mice at the indicated times after BCG infection. Cells were stimulated with PPD for 6 h and intracellular IFN-γ and TNF-α were analyzed by flow cytometry. Each value indicates the percentage of IFN-γ and TNF-α-producing CD4$^+$ T cells. (C) Splenocytes were collected from WT and PD-1$^{-/-}$ mice at 6 and 12 weeks after infection and stained with antibodies to CD4, CD44 and CD62L. The percentage of memory CD4$^+$ T-cell population was analyzed by flow cytometry. Numbers indicate the percentage of CD4$^+$ T cells in each quadrant. (D) Splenocytes were prepared from WT and PD-1$^{-/-}$ mice at the indicated times after infection and stained with anti-CD4 antibody, anti-CD44 antibody and Annexin V. Apoptosis of memory CD4$^+$ T cells (CD44^{high} CD4$^+$ T cells) was measured by Annexin V binding. Shaded histograms, naïve cells; solid lines, BCG-infected cells. Results are the representative of three independent experiments.

reduced viral loads even in hosts suffering from severe lymphopenia (23, 60). Importantly, blockade of the CTLA-4 co-inhibitory pathway does not enhance protection against infection with these viruses and BCG (23, 61, 62). Therefore, the PD-1–PD-L1 pathway appears to be critically involved in the impairment of protective immunity and blockade of the co-inhibitory signal pathway may be a key to augmentation of protection against persistent infection with various pathogens including mycobacteria. Further studies are needed to understand the complete inhibitory mechanism and the potential application of PD-1 in the therapeutic treatment and vaccination for TB.

Funding

Grant-in-Aid for Scientific Research on Priority Areas from the Ministry of Education, Culture, Sports, Science and Technology, Japan; Grants-in-Aid for Scientific Research from the Japan Society for the Promotion of Science; a Grant-in-Aid for Research on Emerging and Re-emerging Infectious Diseases form the Ministry of Health, Labour and Welfare, Japan; and a research grant from the Waksman Foundation of Japan.

Acknowledgement

We are grateful to Dr Tasuku Honjo (Kyoto University, Kyoto, Japan) for generously providing the PD-1$^{-/-}$ mice used in this study.

Disclosure

The authors have no conflicting financial interests.

References

1 WHO. 2009. Global tuberculosis control: a short update to the 2009 report. WHO, Geneva, Switzerland. Available at: www.who.int/tb/publications/global_report/en.
2 Kaufmann, S. H. E. and McMichael, A. J. 2005. Annulling a dangerous liaison: vaccination strategies against AIDS and tuberculosis. *Nat. Med. Suppl.* 11:S33.
3 Russell, R. G. 2007. Who puts the tubercle in tuberculosis? *Nat. Rev. Microbiol.* 5:39.

4 Boudes, P., Sobel, A., Deforges, L. and Leblic, E. 1989. Disseminated *Mycobacterium bovis* infection from BCG vaccination and HIV infection. *JAMA.* 262:2386.
5 Armbruster, C., Junker, W., Vetter, N. and Jaksch, G. 1990. Disseminated bacille Calmette-Guérin infection in an AIDS patient 30 years after BCG vaccination. *J. Infect. Dis.* 162:1216.
6 Reynes, J., Perez, C., Lamaury, I., Janbon, F. and Bertrand, F. 1989. Bacille Calmette-Guérin adenitis 30 years after immunization in a patient with AIDS. *J. Infect. Dis.* 160:727.
7 Orme, I. M. 1987. The kinetics of emergence and loss of mediator T lymphocytes acquired in response to infection with *Mycobacterium tuberculosis. J. Immunol.* 138:293.
8 Muller, I., Cobbold, S. P., Waldmann, H. and Kafmann, S. H. E. 1987. Impaired resistance to *Mycobacterium tuberculosis* infection after selective in vivo depletion of L3T4$^+$ and Lyt-2$^+$ T cells. *Infect. Immun.* 55:2037.
9 Caruso, A. M., Serbina, N., Klein, E., Triebold, K., Bloom, B. R. and Flynn, J. L. 1999. Mice deficient in CD4 T cells have only transiently diminished levels of IFN-γ, yet succumb to tuberculosis. *J. Immunol.* 162:5407.
10 Mogues, T., Goodrich, M. E., Ryan, L., LaCourse, R. and North, R. J. 2001. The relative importance of T cell subsets in immunity and immunopathology of airborne *Mycobacterium tuberculosis* infection in mice. *J. Exp. Med.* 193:271.
11 Saunders, B. M., Frank, A. A., Orme, I. M. and Cooper, A. M. 2002. CD4 is required for the development of a protective granulomatous response to pulmonary tuberculosis. *Cell. Immunol.* 216:65.
12 Flynn, J. L. and Chan, J. 2001. Immunology of tuberculosis. *Annu. Rev. Immunol.* 19:93.
13 Chen, L. 2004. Co-inhibitory molecules of the B7-CD28 family in the control of T-cell immunity. *Nat. Rev. Immunol.* 4:336.
14 Ishida, Y., Agata, Y., Shibahara, K. and Honjo, T. 1992. Induced expression of PD-1, a novel member of the immunoglobulin gene superfamily, upon programmed cell death. *EMBO J.* 11:3887.
15 Okazaki, T. and Honjo, T. 2007. PD-1 and PD-1 ligands: from discovery to clinical application. *Int. Immunol.* 19:813.
16 Shimatani, K., Nakashima, Y., Hattori, M., Hamazaki, Y. and Minato, N. 2009. PD-1$^+$ memory phenotype CD4$^+$ T cells expressing C/EBPα underlie T cell immunodepression in senescence and leukemia. *Proc. Natl Acad. Sci. USA* 106:15807.
17 Keir, M. E., Butte, M. J., Freeman, G. J. and Sharpe, A. H. 2008. PD-1 and its ligands in tolerance and immunity. *Annu. Rev. Immunol.* 26:677.
18 Yamazaki, T., Akiba, H., Iwai, H. *et al.* 2002. Expression of programmed death 1 ligands by murine T cells and APC. *J. Immunol.* 169:5538.
19 Loke, P. and Allison, J. P. 2003. PD-L1 and PD-L2 are differentially regulated by Th1 and Th2 cells. *Proc. Natl Acad. Sci. USA* 100:5336.
20 Liu, J., Hamrouni, A., Wolowiec, D. *et al.* 2007. Plasma cells from multiple myeloma patients express B7-H1 (PD-L1) and increase expression after stimulation with IFN-γ and TLR ligands via a MyD88-, TRAF6-, and MEK-dependent pathway. *Blood* 110:296.
21 Okazaki, T. and Honjo, T. 2006. The PD-1–PD-L pathway in immunological tolerance. *Trends Immunol.* 27:195.
22 Sharpe, A. H., Wherry, E. J., Ahmed, R. and Freeman, G. J. 2007. The function of programmed cell death 1 and its ligands in regulating autoimmunity and infection. *Nat. Immunol.* 8:239.
23 Barber, D. L., Wherry, E. J., Masopust, D. *et al.* 2006. Restoring function in exhausted CD8 T cells during chronic viral infection. *Nature* 439:682.
24 Day, C. L., Kaufmann, D. E., Kiepiela, P. *et al.* 2006. PD-1 expression on HIV-specific T cells is associated with T-cell exhaustion and disease progression. *Nature* 443:350.
25 Boni, C., Fisicaro, P., Valdatta, C. *et al.* 2007. Characterization of hepatitis B virus (HBV)-specific T-cell dysfunction in chronic HBV infection. *J. Virol.* 81:4215.
26 Urbani, S., Amadei, B., Tola, D. *et al.* 2006. PD-1 expression in acute hepatitis C virus (HCV) infection is associated with HCV-specific CD8 exhaustion. *J. Virol.* 80:11398.
27 Das, S., Suarez, G., Beswick, E. J., Sierra, J. C., Graham, D. Y. and Reyes, V. E. 2006. Expression of B7-H1 on gastric epithelial cells: its potential role in regulating T cells during *Helicobacter pylori* infection. *J. Immunol.* 176:3000.
28 Orme, I. M., Roberts, A. D., Griffin, J. P. and Abrams, J. S. 1993. Cytokine secretion by CD4 T lymphocytes acquired in response to *Mycobacterium tuberculosis* infection. *J. Immunol.* 151:518.
29 Winslow, G. M., Roberts, A. D., Blackman, M. A. and Woodland, D. L. 2003. Persistence and turnover of antigen-specific CD4 T cells during chronic tuberculosis infection in the mouse. *J. Immunol.* 170:2046.
30 Lazarevic, V., Nolt, D. and Flynn, J. L. 2005. Long-term control of *Mycobacterium tuberculosis* infection is mediated by dynamic immune responses. *J. Immunol.* 175:1107.
31 Lutz, M. B., Kukutsch, N., Ogilvie, A. L. J. *et al.* 1999. An advanced culture method for generating large quantities of highly pure dendritic cells from mouse bone marrow. *J. Immunol. Meth.* 223:77.
32 Flynn, J. L., Goldstein, M. M., Triebold, K. J., Koller, B. and Bloom, B. R. 1992. Major histocompatibility complex class I-restricted T cells are required for resistance to *Mycobacterium tuberculosis* infection. *Proc. Natl Acad. Sci. USA* 89:12013.
33 Behar, S. M., Dascher, C. C., Grusby, M. J., Wang, C. R. and Brenner, M. B. 1999. Susceptibility of mice deficient in CD1D or TAP1 to infection with *Mycobacterium Tuberculosis. J. Exp. Med.* 189:1973.
34 Darrah, P. A., Patel, D. T., De Luca, P. M. *et al.* 2007. Multifunctional TH1 cells define a correlate of vaccine-mediated protection against Leishmania major. *Nat. Med.* 13:843.
35 Sun, Y., Santra, S., Schmitz, J. E., Roederer, M. and Letvin, N. L. 2008. Magnitude and quality of vaccine-elicited T-cell responses in the control of immunodeficiency virus replication in rhesus monkeys. *J. Virol.* 82:8812.
36 Liu, J., O'Brien, K. L., Lynch, D. M. *et al.* 2009. Immune control of an SIV challenge by T-cell-based vaccine in rhesus monkeys. *Nature* 457:87.
37 Quinn, K. M., Mchugh, R. S., Rich, F. J. *et al.* 2006. Inactivation of CD4$^+$CD25$^+$ regulatory T cells during early mycobacterial infection increases cytokine production but does not affect pathogen load. *Immunol. Cell Biol.* 84:467.
38 Kursar, M., Koch, M., Mittrücker, H. *et al.* 2007. Cutting edge: regulatory T cells prevent efficient clearance of Mycobacterium Tuberculosis. *J. Immunol.* 178:2661.
39 Scott-Browne, J. P., Shafiani, S., Tucker-Heard, G. *et al.* 2007. Expansion and function of Foxp3-expressing T regulatory cells during tuberculosis. *J. Exp. Med.* 204:2159.
40 Boussiotis, V. A., Tsai, E. Y., Yunis, E. J. *et al.* 2000. IL-10-producing T cells suppress immune responses in anergic tuberculosis patients. *J. Clin. Invest.* 105:1317.
41 Bhatt, K., Uzelac, A., Mathur, S., McBride, A., Potian, J. and Salgame, P. 2009. B7 costimulation is critical for host control of chronic *Mycobacterium tuberculosis* infection. *J. Immunol.* 182:3793.
42 Sedy, J. R., Gavrieli, M., Potter, K. G. *et al.* 2005. B and T lymphocyte attenuator regulates T cell activation through interaction with herpes virus entry mediator. *Nat. Immunol.* 6:90.
43 Rohde, K., Yates, R. M., Purdy, G. E. and Russell, D. G. 2007. *Mycobacterium tuberculosis* and the environment within the phagosome. *Immunol. Rev.* 219:37.
44 Lazarevic, V. and Martinon, F. 2008. Linking inflammasome activation and phagosome maturation. *Cell Host Microbe.* 3:199.
45 Pieters, J. 2008. *Mycobacterium tuberculosis* and the macrophages: maintaining a balance. *Cell Host Microbe.* 3:399.
46 Porcelli, S. A. and Jacobs, W. R., Jr. 2008. Tuberculosis: unsealing the apoptotic envelope. *Nat. Immunol.* 9:1101.
47 Jurado, J. O., Alvarez, I. B., Pasquinelli, V. *et al.* 2008. Programmed death (PD)-1:PD-ligand 1/PD-ligand 2 pathway inhibits T cell effector functions during human tuberculosis. *J. Immunol.* 181:116.
48 Hess, J., Miko, D., Catic, A., Lehmensiek, V., Russel, D. G. and Kaufmann, S. H. E. 1998. *Mycobacterium bovis* bacille Calmette-Guérin strains secreting listeriolysin of Listeria monocytogenes. *Proc. Natl Acad. Sci. USA* 95:5299.
49 Billeskov, R., Vingsbo-Lundberg, C., Andersen, P. and Dietrich, J. 2007. Induction of CD8 T cells against a novel epitope in TB10.4:

correlation with mycobacterial virulence and the presence of a functional region of defference-1. *J. Immunol.* 179:3973.
50 Ngai, P., McCormick, S., Small, C. *et al.* 2007. Gamma interferon responses of CD4 and CD8 T-cell subsets are quantitatively different and independent of each other during pulmonary *Mycobacterium bovis* BCG infection. *Infect. Immun.* 75:2244.
51 Freeman, G. J., Long, A. J., Iwai, Y. *et al.* 2000. Engagement of the PD-1 immunoinhibitory receptor by a novel B7 family member leads to negative regulation of lymphocyte activation. *J. Exp. Med.* 192:1027.
52 Brodin, P., Majlessi, L., Marsollier, L. *et al.* 2006. Dissection of ESAT-6 system 1 of *Mycobacterium tuberculosis* and impact on immunogenicity and virulence. *Infect. Immun.* 74:88.
53 Sable, S. B., Kalra, M., Verma, I. and Khuller, G. K. 2007. Tuberculosis subunit vaccine design: the conflict of antigenicity and immunogenicity. *Clin. Immunol.* 122:239.
54 Erb, K. J., Kirman, J., Delahunt, B., Chen, W. and Le Gros, G. 1998. IL-4, IL-5 and IL-10 are not required for the control of *M. bovis*-BCG infection in mice. *Immunol. Cell Biol.* 76:41.
55 Murray, P. J. and Young, R. A. 1999. Increased antimycobacterial immunity in interleukin-10-deficient mice. *Infect. Immun.* 67:3087.
56 Mason, C. M., Porretta, E., Zhang, P. and Nelson, S. 1999. $CD4^+CD25^+$ transforming growth factor-β-producing T cells are present in the lung in murine tuberculosis and may regulate the host inflammatory response. *Clin. Exp. Immunol.* 148:537.
57 Forbed, E. K., Sander, C., Ronan, E. O. *et al.* 2008. Multifunctional, high-level cytokine-producing Th1 cells in the lung, but not spleen, correlate with protection against *Mycobacterium tuberculosis* aerosol challenge in mice. *J. Immunol.* 181:4955.
58 Homann, D., Teyton, L. and Oldstone, M. B. A. 2001. Differential regulation of antiviral T-cell immunity results in stable $CD8^+$ but declining $CD4^+$ T-cell memory. *Nat. Med.* 7:913.
59 Hataye, J., Moon, J. J., Khoruts, A., Reilly, C. and Jenkins, M. K. 2006. Naïve and memory $CD4^+$ T cell survival controlled by clonal abundance. *Science* 312:114.
60 Velu, V., Titanji, K., Zhu, B. *et al.* 2009. Enhancing SIV-specific immunity *in vivo* by PD-1blockade. *Nature* 458:206.
61 Cecchinato, V., Tryniszewska, E., Ma, Z. M. *et al.* 2008. Immune activation driven by CTLA-4 blockade augments viral replication at mucosal sites in simian immunodeficiency virus infection. *J. Immunol.* 180:5439.
62 Kirman, J., McCoy, K., Hook, S. *et al.* 1999. CTLA-4 blockade enhances the immune responses induced by mycobacterial infection but does not lead to increased protection. *Infect. Immun.* 67:3786.

J. Biochem. 2010;148(5):593–602 doi:10.1093/jb/mvq093

JB THE JOURNAL OF BIOCHEMISTRY

A revised biosynthetic pathway for phosphatidylinositol in Mycobacteria

Received June 30, 2010; accepted August 11, 2010; published online August 26, 2010

Hiroyuki Morii[1,*], Midori Ogawa[2], Kazumasa Fukuda[2], Hatsumi Taniguchi[2] and Yosuke Koga[1]

[1]Department of Chemistry and [2]Department of Microbiology, University of Occupational and Environmental Health, Japan, 1-1 Iseigaoka, Yahatanishi-ku, Kitakyushu, 807-8555, Japan

*Hiroyuki Morii, Department of Chemistry, University of Occupational and Environmental Health, Japan, 1-1 Iseigaoka, Yahatanishi-ku, Kitakyushu, 807-8555, Japan.
Tel: +81 93 603 1611, Fax: +81 93 693 9921,
email: h-morii@health.uoeh-u.ac.jp

For the last decade, it has been believed that phosphatidylinositol (PI) in mycobacteria is synthesized from free inositol and CDP-diacylglycerol by PI synthase in the presence of ATP. The role of ATP in this process, however, is not understood. Additionally, the PI synthase activity is extremely low compared with the PI synthase activity of yeast. When CDP-diacylglycerol and [^{14}C]1L-*myo*-inositol 1-phosphate were incubated with the cell wall components of *Mycobacterium smegmatis*, both phosphatidylinositol phosphate (PIP) and PI were formed, as identified by fast atom bombardment-mass spectrometry and thin-layer chromatography. PI was formed from PIP by incubation with the cell wall components. Thus, mycobacterial PI was synthesized from CDP-diacylglycerol and *myo*-inositol 1-phosphate via PIP, which was dephosphorylated to PI. The gene-encoding PIP synthase from four species of mycobacteria was cloned and expressed in *Escherichia coli*, and PIP synthase activity was confirmed. A very low, but significant level of free [^{3}H]inositol was incorporated into PI in mycobacterial cell wall preparations, but not in recombinant *E. coli* cell homogenates. This activity could be explained by the presence of two minor PI metabolic pathways: PI/inositol exchange reaction and phosphorylation of inositol by ATP prior to entering the PIP synthase pathway.

Keywords: inositol/phosphatidylinositol phosphate synthase/phospholipid/*Mycobacterium smegmatis*/tuberculosis.

Abbreviations: AI, archaetidylinositol; AIP, archaetidylinositol phosphate; CDP-DAG, CDP-diacylglycerol; FAB-MS, fast atom bombardment-mass spectrometry; PI, phosphatidylinositol: PIP, phosphatidylinositol phosphate; TLC, thin-layer chromatography.

Mycobacterium tuberculosis is a major causative agent of mortality worldwide. *M. tuberculosis* has developed resistance to every new drug used to treat tuberculosis, resulting in the recent global emergence of drug-resistant tuberculosis (*1*).

All mycobacterial cells have lipid-rich cell envelopes, which are the basis of resistance to macrophages or anti-bacterial drugs (*2*). Recent studies revealed that the cell wall constituent lipoarabinomannan and its precursors, phosphatidylinositol (PI) mannosides, have an important role in the growth of mycobacterial cells and their infectivity (*2–9*). Therefore, the biosynthesis of cell wall lipids is a promising target of anti-mycobacterial drugs.

The first step of lipoarabinomannan biosynthesis is the formation of the starting material PI. Salman *et al.* (*10*) reported that PI is synthesized by mycobacterial cell wall constituents from CDP-diacylglycerol (CDP-DAG) and free inositol in the presence of ATP. The role of ATP in the reaction, however, is not understood (*10*). The proposed pathway for mycobacteria was the same as that of eukaryotes. Eukaryotic PI is synthesized from CDP-DAG and *myo*-inositol (*11*), which is generated from D-glucose 6-phosphate (*12*, *13*).

$$\text{D-glucose-6-phosphate} \rightarrow \text{1L-}myo\text{-inositol 1-phosphate} \quad (1)$$

$$\text{1L-}myo\text{-inositol 1-phosphate} \rightarrow myo\text{-inositol} + \text{Pi} \quad (2)$$

$$myo\text{-inositol} + \text{CDP-diacylglycerol} \rightarrow \text{phosphatidyl-}myo\text{-inositol} + \text{CMP} \quad (3)$$

Reactions (1) and (3) are catalysed by 1L-*myo*-inositol 1-phosphate synthase and PI synthase, respectively.

Over the last several years, we have investigated the *in vitro* biosynthesis of an ether-type inositol phospholipid (archaetidyl-*myo*-inositol) in methanoarchaea. We determined that little inositol is incorporated into lipids, whereas inositol 1-phosphate is a good substrate. Based on the archaeal-enzyme study, we re-examined the PI synthase reaction in mycobacteria because of the reported low-specific activity and the presence of ATP in the reaction mixture. ATP is not required for the eukaryotic PI synthase reaction. The

specific activity of [^{3}H] inositol incorporation reported by Jackson *et al.* (*14*) was 2.5 pmol/h/mg protein in mycobacterial cell walls. This corresponds to 0.014% of the specific activity (18 nmol/h/mg protein) in *Saccharomyces cerevisiae* cell homogenates (*15*).

We recently reported a novel biosynthetic pathway of archaetidylinositol (AI) in the cells of the methanoarchaeon *Methanothermobacter thermautotrophicus* (*16*). The reaction sequence in the archaeon after reaction (1) is as follows:

CDP-archaeol + 1L-*myo*-inositol 1-phosphate → archaetidyl-*myo*-inositol phosphate + CMP (4)

archaetidyl-*myo*-inositol phosphate → archaetidyl-*myo*-inositol + Pi (5)

In a mycobacterial cell-free system with the reaction mixture containing inositol 1-phosphate and CDP-DAG without ATP, we detected activity comparable to that of yeast homogenates. The use of a different substrate for PI synthesis led to the discovery of a novel PI-biosynthetic pathway. The present article describes a novel-biosynthetic pathway of PI in mycobacteria via phosphatidylinositol phosphate (PIP) as in AI synthesis in methanoarchaea. In addition to this main *de novo* synthesis of PI, we also detected a PI/inositol exchange reaction and inositol phosphorylation activity. These reactions complicate the experimental results obtained using crude enzyme preparations of the PI metabolism in mycobacteria.

Because of the difference in the PI biosynthetic mechanism in mycobacteria compared to that of Eucarya, this pathway might be a promising target for drug discovery.

Experimental Procedures

Materials

β-D-Glucose 6-phosphate was purchased from Sigma-Aldrich (Tokyo, Japan). [^{14}C(U)]Glucose 6-phosphate (3.7 MBq/ml) was obtained from Moravek Biochemicals, Inc. (Brea, CA, USA). [2-^{3}H]*myo*-Inositol (37 MBq/ml) was obtained from MP Biomedicals, LLC. (Santa Ana, CA, USA). [^{14}C]Inositol 1-phosphate, which was not commercially available, was prepared from [^{14}C(U)]glucose 6-phosphate using *myo*-inositol phosphate synthase from *M. thermautotrophicus* and filtered with an Ultrafilter (USY-1 M = 10,000, Advantec), as described earlier (*16*). The filtrate contained [^{14}C]inositol 1-phosphate, unreacted [^{14}C]glucose 6-phosphate, and other low-molecular weight compounds. This filtrate (hereafter referred to as [^{14}C]inositol 1-phosphate) was used without further purification as a substrate for the PIP synthase reaction. CDP-dipalmitoylglycerol [CDP-DAG(dipalmitoyl)] and CDP-dioleoylglycerol [CDP-DAG(dioleoyl)] were chemically synthesized from 1,2-dipalmitoyl-*sn*-glycero-3-phosphate (Avanti Polar Lipids Inc., Alabaster, AL, USA) and 1,2-dioleoyl-*sn*-glycero-3-phosphate (Avanti Polar Lipids Inc.), respectively, as described earlier (*17*). PI (soybean) was obtained from DOOSAN Serdary Research Laboratories (Toronto, ON, USA). Percoll was obtained from GE Healthcare (Piscataway, NJ, USA). Dowex AG1 (X8; 100–200 mesh, chloride form; BIO RAD, Berkeley, CA, USA) was converted to the formate form. *Mycobacterium smegmatis* mc^{2}155, *M. bovis* BCG, *M. marinum* (clinical isolate) and *M. chelonae* subsp. *abscessus* (JATA63-1) were used in this study.

Preparation of standard PIP

The recombinant AI phosphate (AIP) synthase expressed in *Escherichia coli* cells (*16*) had significant activity (~20%) with CDP-DAG(dioleoyl) was used as the substrate instead of CDP-archaeol. The products of this reaction were confirmed as PIP and a small amount of PI. The product was used as standard PIP.

Growth of microorganisms

Mycobacterium smegmatis mc^{2}155 cells were grown in Difco Nutrient Broth (Becton Dickinson, Franklin Lakes, NJ, USA) for ~2 days while shaking at 37°C and harvested by centrifugation. Cells were washed with buffer A (50 mM MOPS [pH 7.9] containing 10 mM $MgCl_2$ and 5 μM 2-mercaptoethanol). The pelleted cells were stored at −20°C until use.

Preparation of crude cell wall, cytosolic, membrane and cell wall fractions

Frozen cells (~4 g wet weight) of *M. smegmatis* were thawed in 20 ml buffer A (see above) and disrupted by sonication using a SONIFIER 250 (1 cm probe; Branson, Danbury, CT, USA) for 10 min (10 × 60 s pulses with 90-s cooling intervals between pulses) as described by Salman *et al.* (*10*). Crude cell walls were obtained by centrifugation of the above whole sonicate as described by Jackson *et al.* (*14*). Cytosolic and membrane fractions were separated by centrifugation of the 27,000*g*-supernatant at 100,000*g* for 1 h (*10*). The cell wall fraction was purified from the re-suspended 27,000*g*-pellet in buffer A by centrifugation in 60% Percoll at 27,000*g* for 1 h (*10*, *18*). The upper one-third layer of the centrifuge tube was saved as the purified cell wall fraction (hereafter called cell walls). The crude cell wall, cytosolic, membrane and purified cell wall fractions were stored at −20°C until use.

Measurement of PIP synthase activity

The complete assay mixture (final volume, 0.2 ml) contained 50 μl of [^{14}C]inositol 1-phosphate (19 nmol, 2800 Bq), 40 nmol CDP-DAG, 50 mM MOPS buffer (pH 7.9), 10 mM $MgCl_2$, 5 μM 2-mercaptoethanol, 0.4% (w/v) CHAPS and the cell wall fraction (200 μg protein) of *M. smegmatis* cell homogenate. In some experiments, the homogenates of *E. coli* pET21a-PIPS, in which the gene-encoding-PIP synthase of one of *Mycobacterium* species (see below) had been expressed, was used instead of the cell walls. CDP-DAG was dispersed with the aqueous components of the reaction mixture except for CHAPS, [^{14}C]inositol 1-phosphate, and the enzyme preparation in a 1.5-ml microtube by continuous sonication at room temperature for 15 min using a Bransonic 1210 (Branson) bath. After the addition of CHAPS, [^{14}C]inositol 1-phosphate, and the enzyme preparation, the reaction mixture was incubated at 37°C for 1 h. The reaction was stopped by adding 1 ml of 0.1 M HCl in methanol and the mixture was transferred to a 10-ml Teflon-lined, screw-capped glass tube with 1.5 ml of 0.1 M HCl in methanol and 2.5 ml $CHCl_3$. Finally, 2.15 ml of 1 M $MgCl_2$ (pH 2) was added to the mixture to partition the reactants and the products into aqueous and organic layers. After washing twice with 0.1 M HCl/methanol-1 M $MgCl_2$ (pH 2) (1 : 0.8, v/v), the organic layer was evaporated to dryness and the radioactivity in the fraction was counted. PIP-synthase activity was expressed as nano mol of (PIP + PI)/h. Because PI is derived from PIP as described below, (PIP + PI) represents the total PIP synthesized.

Measurement of free inositol incorporation into lipid

Incorporation of free inositol into lipid was measured by essentially the same method used in Salman *et al.* (*10*). The complete reaction mixture (final volume, 0.2 ml) comprising 2.5 μM [^{3}H]inositol (0.5 nmol, 74 kBq/Assay), 40 nmol CDP-DAG, 50 mM MOPS buffer (pH 7.9), 10 mM $MgCl_2$, 5 μM 2-mercaptoethanol, 0.1 mM ATP, 5 mM glucose, 0.4% (w/v) CHAPS and the cell wall fraction (200 μg protein) of *M. smegmatis* cell homogenates, was incubated at 37°C for 1 h and extracted with the same procedure described to measure the PIP-synthase activity.

Acid extraction of lipid from enzyme reaction mixtures or silica gel scraped from a TLC plate

Lipids were extracted from the enzyme reaction mixtures or silica gel scraped from a preparative-TLC plate by the acidic Bligh and Dyer